Heliyon 10 (2024) e39378

Contents lists available at ScienceDirect

Heliyon

journal homepage: www.cell.com/heliyon

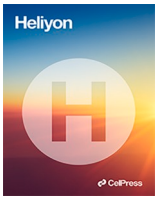

Research article

Unveiling mitochondria as central components driving cognitive decline in alzheimer's disease through cross-transcriptomic analysis of hippocampus and entorhinal cortex microarray datasets

Pajaree Sonsungsan [a], Supatha Aimauthon [b,c], Nattawet Sriwichai [d], Poommaree Namchaiw [e,f,*]

[a] *Mathematics and Statistics, School of Science, Walailak University, Nakhon Si Thammarat, Thailand*
[b] *Chemical Engineering, Faculty of Engineering, King Mongkut's University of Technology Thonburi, Bangkok, Thailand*
[c] *Center for Biologics Research and Development, Chulabhorn Research Institute, Bangkok, Thailand*
[d] *Center for Agricultural Systems Biology, Pilot Plant Development and Training Institute, King Mongkut's University of Technology Thonburi (Bang Khun Thian), Bangkok, Thailand*
[e] *Biological Engineering Program, Faculty of Engineering, King Mongkut's University of Technology Thonburi, Bangkok, Thailand*
[f] *Neuroscience Center for Research and Innovation, Learning Institute, King Mongkut's University of Technology Thonburi, Bangkok, Thailand*

ARTICLE INFO

Keywords:
Alzheimer's disease
Microarray
Synaptic vesicle
Cytoskeleton
Mitochondria

ABSTRACT

Alzheimer's disease (AD) is a prevalent neurodegenerative disorder characterized by symptoms such as memory loss and impaired learning. This study conducted a cross-transcriptomic analysis of AD using existing microarray datasets from the hippocampus (HC) and entorhinal cortex (EC), comparing them with age-matched non-AD controls. Both of these brain regions are critical for learning and memory processing and are vulnerable areas that exhibit abnormalities in early AD. The cross-transcriptomic analysis identified 564 significantly differentially expressed genes in HC and 479 in EC. Among these, 151 genes were significantly differentially expressed in both tissues, with functions related to synaptic vesicle clustering, synaptic vesicle exocytosis/endocytosis, mitochondrial ATP synthesis, hydrogen ion transmembrane transport, and structural constituent of cytoskeleton, suggesting a potential association between cognitive decline in AD, synaptic vesicle dynamics, dysregulation of cytoskeleton organization, and mitochondrial dysfunction. Further gene ontology analysis specific to the HC revealed the gene ontology enrichment in aerobic respiration, synaptic vesicle cycle, and oxidative phosphorylation. The enrichment analysis in CA1 of HC revealed differentiation in gene expression related to mitochondrial membrane functions involved in bioenergetics, mitochondrial electron transport, and biological processes associated with microtubule-based process, while analysis in the EC region showed enrichment in synaptic vesicle dynamics which is associated with neurotransmitter release and the regulation of postsynaptic membrane potential and synaptic transmission of GABAergic and glutamatergic synapse. Protein-protein interaction analysis highlighted central hub proteins predominantly expressed in mitochondria, involved in regulation of oxidative stress and ATP synthesis. These hub proteins interact not only within the mitochondria but also with proteins in

* Corresponding author. Biological Engineering Program, Faculty of Engineering, King Mongkut's University of Technology Thonburi, Bangkok, Thailand.
E-mail address: poommaree.nam@mail.kmutt.ac.th (P. Namchaiw).

https://doi.org/10.1016/j.heliyon.2024.e39378
Received 21 May 2024; Received in revised form 9 October 2024; Accepted 13 October 2024
Available online 15 October 2024

the vesicular membrane and neuronal cytoskeleton, indicating a central role of mitochondria. This finding underscores the association between clinical symptoms and mitochondrial dysregulation of synaptic vesicle dynamics, cytoskeleton organization, and mitochondrial processes in both the HC and EC of AD. Therefore, targeting these dysregulated pathways could provide promising therapeutic targets aimed at cognitive decline and memory impairment in early AD stages.

1. Introduction

Alzheimer's disease (AD) is a prevalent neurodegenerative disorder affecting the elderly population worldwide. The global estimation predicted that the number of individuals afflicted by dementia would increase to 152.8 million by the year 2050 [1]. The primary contributor to dementia in the elderly is AD, in which the changes within the brain begin in the absence of noticeable symptoms. As the disease progresses, patients often develop dementia, leading to memory loss and the inability to learn new information [2]. These symptoms significantly hamper their daily lives and facing life-threatening challenges.

The symptoms vary between individuals, making early diagnosis challenging [3]. Several continuing efforts aim to study the pathophysiological mechanisms underlying the disease. Currently, numerous drugs are in various stages of clinical trials and development [4,5]. However, the precise cause of AD remains elusive, contributing to a high failure rate in clinical trials for several drug development initiatives [6].

Previous studies have unveiled the accumulation of extracellular amyloid-beta (Aβ) plaques and intracellular tau tangles as the primary pathological hallmarks of AD, along with other hallmarks such as cytoskeletal, mitochondrial, and synaptic dysfunction [7,8]. Amyloid plaque, as known as senile plaques, represents abnormal deposits of Aβ protein outside of neurons. Aβ aggregation may contribute to the formation of neurofibrillary tangles (NFTs) which are the abnormal aggregations of phosphorylated-tau protein that form inside neurons. Normally, tau protein plays a role in stabilizing microtubules, which are essential for the structure and function of neurons. However, the hyperphosphorylation of tau protein leads to insoluble paired helical filaments (PHFs) and straight filaments (SFs) which then form NFTs. The severity of AD is often classified using systems such as Braak staging, which describes the progression of AD based on the distribution and severity of NFTs in the brain. It ranges from early stages (I-II), where NFTs are primarily confined to the transentorhinal region, to intermediate (III-IV), where NFTs spread to the limbic system, and finally to advanced stages (V-VI), characterized by widespread distribution of NFTs throughout the hippocampus and other neocortical areas [9]. The abnormal accumulations of Aβ disrupt neuronal function and ultimately lead to cell death. Therefore, the amyloid cascade hypothesis has been proposed as a central theory of AD pathogenesis. According to the amyloid hypothesis, the clinical course of AD begins with the accumulation of Aβ then followed by neuroinflammation, phosphorylated-tau protein accumulation, brain metabolism dysfunction, and cognitive decline [5]. Aβ plaques and NFTs collectively drive AD progression and thus are targeted for pharmaceutical development. Alongside these hallmarks, dysfunctions of the neuronal cytoskeleton, mitochondria, synaptic formation, and neurotransmitter system, neuroinflammation, and vascular factors are recently recognized as prominent targets for AD [4,5].

Besides the conventional amyloid hypothesis, the mitochondrial cascade hypothesis has recently been promoted as a new thought of AD pathogenesis [10]. There is evidence showing that Aβ accumulates over decades before symptoms of Alzheimer's disease arise [11]. This suggests that the presence of Aβ accumulation may not necessarily lead directly to neurodegeneration. Besides, Aβ slowly accumulate and tend to become plateau as AD progressed [11]. This indicated that the amyloid cascade alone may not explain the clinical symptoms. Emerging research has highlighted multiple connections between AD's clinical features and mitochondrial dysfunction. Khan and colleagues, therefore, proposed that mitochondria could be a pivotal component altering brain metabolic rates and accelerating Aβ accumulation [10]. Although the role of mitochondrial dysfunction as a cause or consequence of AD remains debated, previous evidence strongly implicates mitochondrial dysfunction in AD progression. Furthermore, mitochondria play critical roles in cellular processes such as bioenergetics, calcium homeostasis, oxidative stress control, and apoptosis regulation. Thus, targeting mitochondrial function represents a promising therapeutic approach for intervening in AD and addressing key aspects of cellular dysfunction implicated in disease progression.

Several researches have consistently shown the structural and functional abnormalities in the hippocampus (HC) and entorhinal cortex (EC) regions even in the early stages of the condition. These regions play critically roles in memory formation and retrieval. Therefore, these pathological changes in HC and EC contribute to AD characteristic such as memory impairment and cognitive decline [12–14]. Neurons in these regions are particularly vulnerable and are among the first to exhibit abnormalities in early AD stages, highlighting the relevance of gene expression in HC and EC neurons to patient's symptoms. In recent decades, bioinformatics analysis including mathematical and statistical techniques have emerged as powerful tools for obtaining gene expression profiles and identify the differential expressed genes (DEGs) [15]. Microarray technology has provided an extensive database for obtaining gene expression profiles from multiple research laboratories, offering insights into DEGs in AD patients versus healthy individuals. In this study, we conducted cross-transcriptomic analysis using multiple existing microarray datasets to identify DEGs in HC and EC tissues from AD patients compared to healthy individuals. We retrieved five microarray datasets (GSE36980, GSE1297, GSE28146, GSE48350, and GSE5281) from the Gene Expression Omnibus (GEO) public database [16], specifically targeting HC and EC tissue analysis by using the keyword "Alzheimer's". The results for the EC were obtained from GSE48350 and GSE5281, while HC results were obtained from two subregions. GSE36980 and GSE48350 were collected from undefined region of the HC, whereas GSE1297, GSE28146, and GSE5281 focused specifically on the CA1 subregion. The variations in tissue collection, experimental methods, and microarray platforms can

introduce study-specific biases. Therefore, in this study, we performed a cross-transcriptomics analysis of multiple microarray datasets to identify genes that consistently show differential expression across studies, while accounting for tissue differences.

2. Materials and methods

2.1. Microarray dataset selection and collection

Gene expression datasets of human brain tissue from healthy samples and AD patients were obtained from the NCBI's Gene Expression Omnibus (GEO database; https://www.ncbi.nlm.nih.gov/geo/). We focused on the experiment that measured expression profiles of genes in the HC and EC tissues from post-mortem human brain tissues. To retrieve gene expression data, we meticulously searched the GEO database using the keywords "Alzheimer's, hippocampus, and entorhinal cortex". We specifically targeted the datasets characterized by "expression profiling by array" in *Homo sapiens* only. Consequently, five microarray array datasets were collected including GSE36980 [17], GSE1297 [18], GSE28146 [19], GSE48350 [20], and GSE5281 [21]. Samples in GSE36980 were subjected to microarray analysis using the GeneChip Human Gene 1.0 ST array (GPL6244) (Affymetrix, Santa Clara, CA, USA), which consisted of 33,297 probes. Samples in GSE1297 were detected based on Affymetrix Human Genome U133A Array (GPL96), which consisted of 22,283 probes. The remaining subjected samples used Affymetrix Human Genome U133 Plus 2.0 Array (GPL570), which contained 54,675 probes. The gene expression data of the HC tissues were retrieved from GSE36980 (8 AD patients and 10 non-AD patients), GSE1297 (22 AD patients and 9 non-AD patients), GSE5281 (10 AD patients and 13 non-AD patients), GSE28146 (22 AD patients and 8 non-AD patients), and GSE48350 (19 AD patients and 43 non-AD patients). The gene expression data of the EC tissues were retrieved from GSE5281 (10 AD patients and 13 non-AD patients) and GSE48350 (19 AD patients and 43 non-AD patients). The summarized details of selected datasets are described in Supplementary File 1.

2.2. Data processing

We downloaded the raw data (CEL files) of each dataset from the GEO database (https://www.ncbi.nlm.nih.gov/geo/) and read the CEL files using the ReadAffy function from the GEOquery library in R (version 4.1.3) [22]. Each dataset was normalized with the robust multi-average (RMA) method using the rma function from the affy package [23]. The RMA method is the most widely used pre-processing algorithm for Affymetrix gene expression microarrays which performs background corrected, normalized, and summarized expression data [24]. After the normalization, each probe was mapped to a gene symbol. For a gene that has more than one probe, we chose the median to represent the expression of the gene. Next, samples in each dataset were clustered based on their Euclidean distance using the hierarchical clustering function, hclust, from the WGCNA package [25]. A dendrogram of a sample tree was plotted to detect outlier samples. Outlier samples were removed from the datasets for further analysis. To assess the similarity between samples within and across groups, the gene expression matrices were then subjected to perform a principal component analysis (PCA) using the prcomp function in R (version 4.1.3) [26]. Notably, AD stages in datasets GSE28146 and GSE1297 were categorized as incipient, moderate, and severe stage. While the GSE48350 dataset employed a classification based on Braak stages (III-VI) to define AD samples [20]. It is essential to highlight that due to the limited availability of datasets categorized by Braak stages, we refrained from conducting a differential gene expression analysis specifically between these Braak stages. Instead, we aggregated all AD Braak stages III-VI as representative of AD samples for this study. This decision was made by the definition of Braak stages, where stages III or more signify the presence of NFTs in the EC and HC, while higher Braak stages correspond to the involvement of additional brain regions such as neocortex [9]. Consequently, all Braak stages were collectively considered as AD samples in our analysis.

2.3. Differential gene expression analysis

The screening of Differential Expressed Genes (DEGs) was performed by using the Limma package in R [27]. The Benjamini-Hochberg procedure (FDR) was used to control the expected proportion of false discoveries of multiple hypothesis testing. The criteria for significant DEGs are adjusted p-value less than 0.05 (FDR <0.05) and the absolute of the log 2-fold change more than 0.5 ($|\text{Log2 FC}| > 0.5$). The significant genes were combined from all datasets for the HC and EC tissue, separately. The overlapped DEGs from both tissues were then identified using Venn diagram webtool (http://bioinformatics.psb.ugent.be/webtools/Venn/). The results of down-regulated and up-regulated DEGs are shown in the diagram separately.

2.4. Gene ontology enrichment and KEGG pathway analysis

Down- and up-regulated significant DEGs from same tissue were further performed the gene ontology (GO) analysis based on biological process (BP), cellular component (CC), and molecular function (MF) terms by using the public web server DAVID 2024 (https://david.ncifcrf.gov/) [28]. Specifically, the analysis was restricted to the significance GO terms of EASE Score or a modified Fisher Exact p-value less than 0.05. The results were visualized as bubble diagrams. Significant genes were further identified in the KEGG pathway database (https://www.genome.jp/kegg/) of Alzheimer's disease to identify the function and pathway that play a role in Alzheimer's disease [29].

2.5. PPI network analysis

The Protein-protein interaction (PPI) network analysis was performed using the online database Cytoscape/StringApp [30], which is an application for visualizing networks and pathways to help interpret the interaction and relationship between significant genes. The PPI network of the DEGs was retrieved from the STRING database version 12.0 (https://string-db.org/) [31]. The network was performed under the setting of the significant interaction among genes by a medium confidence score of more than 0.7 and FDR of less than 0.05.

3. Results

3.1. Data collection and preprocessing

This study involved collecting and preprocessing gene expression datasets to identify significantly expressed genes associated with AD in the HC and the EC from the GEO database [16]. An overview of the workflow is depicted in Fig. 1. The microarray database was assembled using the keywords "Alzheimer's" from human HC and EC samples. We retrieved five GSE datasets including GSE36980, GSE1297, GSE28146, GSE48350, and GSE5281. Each dataset conducted microarray on postmortem brain tissue obtained from four

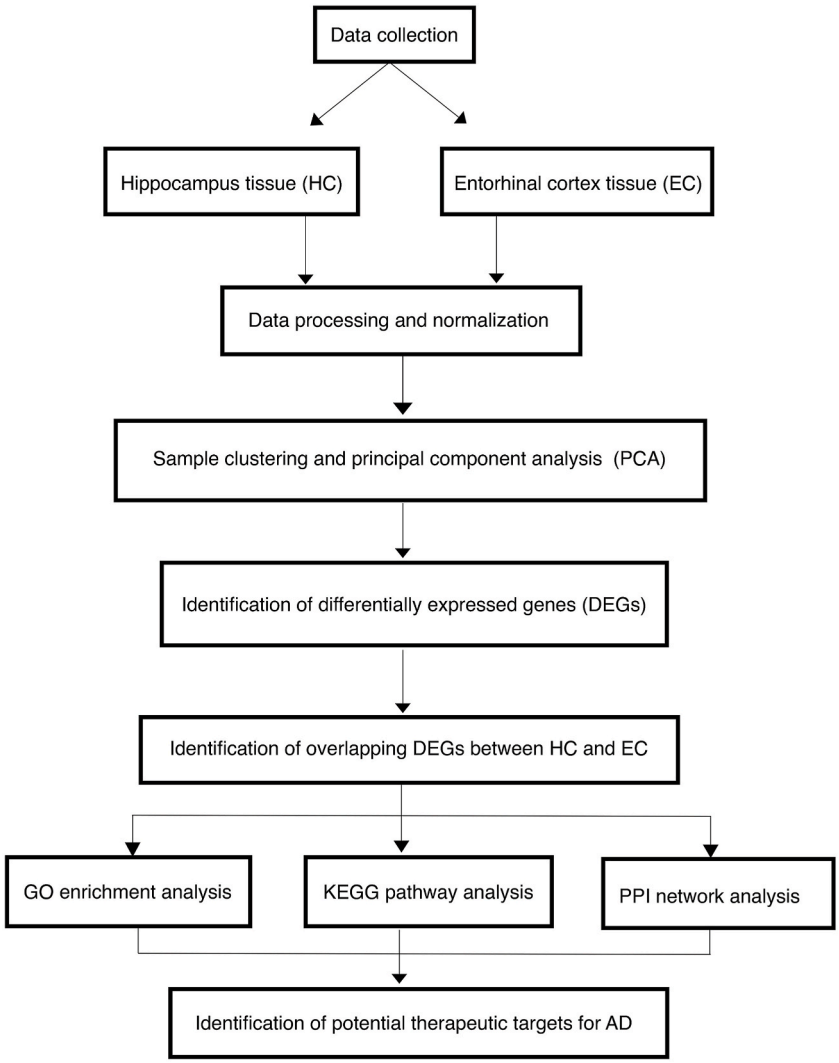

Fig. 1. Flowchart of the analysis procedure. The public microarray raw data specific to HC and EC tissues were downloaded and performed data processing. Normalization was performed, followed by grouping into AD and non-AD categories for each dataset. Sample clustering and principal component analysis (PCA) were applied to detect outlier samples. The differential gene expression between AD versus non-AD or advanced AD stage versus middle and early stages was analyzed. Significant genes were identified from multiple experiments and then underwent gene ontology (GO) enrichment, KEGG pathway analysis, and PPI network construction. Finally, the target genes for AD that specific to HC and EC were identified.

different resources: Fukuoka (GSE36980), Kentucky (GSE1297 and GSE28146), California (GSE48350), and Arizona (GSE5281) [16]. The AD samples were characterized by either Mini Mental Status Examination (MMSE), Braak stage, or Consortium to Establish a Registry for Alzheimer's Disease (CERAD) guideline (refer to Supplementary File 1). We observed that all AD samples were characterized by a Braak stage of III or higher, indicating the presence of NFTs in the limbic system, such as the HC and EC. While age is a well-established risk factor for AD, gender also plays a significant role, especially in women. Although the collected data from each study were age-matched, the AD samples contained a higher proportion of females than males, as detailed in Supplementary File 1.

Microarray probe annotation packages specific to the GPL platform were obtained through R Bioconductor as shown in Table 1. During data preprocessing, microarray datasets underwent a series of steps to remove systematic biases before further analysis. In this study, we separately analyzed the dataset for HC and EC tissues using the same manner. In each dataset, probe intensity raw data was transformed into a log2 scale and normalized using the rma function within the Limma package [27] to mitigate non-biological variances among samples. The distribution of gene expression level between raw data and normalized data for each dataset was shown in Fig. 2(A–N). After normalization, gene expression values of multiple probes associated with a single hybridized gene were combined using median values to represent a gene expression profile for a gene. A dendrogram of sample clustering of each dataset was plotted to detect outlier samples. The samples that were substantially different from the other leaves were identified as outliers and were then removed from the datasets Supplementary File 2. The number of the remaining samples in each dataset is shown in Table 1. After preprocessing, each dataset underwent principal components analysis (PCA) to investigate the overall structure of AD and non-AD samples in each dataset (Fig. 3(A–G)). Despite being conducted on different microarray platforms, it is important to note that 30 out of 31 tissue samples from GSE1297 are identical to those in GSE28146, except for the control 1039 sample [32]. The PCA results showed that the first principal component (PC1) has large positive associations with most AD samples in GSE5281 for both tissues. Whereas PC1 has a large negative with most AD samples for GSE48350 for both tissues and for GSE3680. Moreover, we found that the second principal component (PC2) has large positive associations with most AD samples in GSE28146. These results indicated that the AD samples have a correlation between them and differ from the non-AD samples in each dataset. However, AD and non-AD samples in GSE1297 have large positive and negative for both PC1 and PC2. This may be due to the dispersion among the three AD stages, which introduces the heterogeneity and makes it harder to distinguish AD from non-AD samples. Moreover, the small number of non-AD samples may not provide enough variance for clear differentiation.

4. Gene expression profiling Reveals synaptic, cytoskeletal, and mitochondrial dysregulation in the entorhinal cortex and hippocampus of Alzheimer's

HC and EC are two critical brain regions within the limbic system that play crucial roles in learning and memory [33]. Notably, damage to the HC and EC has frequently been associated with memory impairment symptoms in AD [34,35]. Given the importance of these brain regions, this study investigated the molecular alterations of AD by focusing on gene expression alterations within the HC and EC to uncover genes significantly correlated with the pathological relevance of AD. To identify such genes, we carefully analyzed transcriptomic data of AD versus non-AD (GSE36980, GSE48350 and GSE5281) and three AD stages: severe, moderate, and incipient versus each other's (GSE1297 and GSE28146), using the Limma package in R [27], the transcriptome of each brain region were independently analyzed. Significant differentially expressed genes (DEGs) were identified with the criteria of the absolute Log2 fold change more than 0.5 and adjusted p-value less than 0.05 ($|\text{Log2 FC}| > 0.5$, FDR <0.05). A complete list of up-regulated and down-regulated DEGs in each brain subregion can be found in Supplementary File 3. After removing duplicate DEGs, a total of 3766 unique DEGs of AD versus non-AD were identified across five HC datasets (564 DEGs were found in more than one dataset), and 4745 unique DEGs were identified across two EC datasets (479 DEGs were found in more than one dataset). Among these, 151 common DEGs exhibited a similar pattern of expression across both tissue types, with consistent down-regulation of 143 DEGs and up-regulation of 8 DEGs (Table 2, Supplementary File 3). These DEGs were subsequently analyzed by the DAVID 2024 web-based tool (Fig. 4) [28]. Enrichment analysis of these DEGs revealed key biological processes such as "synaptic vesicle clustering", "synaptic vesicle lumen acidification", "synaptic vesicle exocytosis", "synaptic vesicle endocytosis", and "synaptic transmission, GABAergic", highlighting disruptions in neurotransmitter signaling and synaptic plasticity, which can contribute to memory loss and cognitive decline in AD. Most DEGs were involved in the synaptic vesicle priming process, essential for vesicle fusion with the neuronal membrane and neurotransmitter releasing (Fig. 5). Additionally, enrichment in GABAergic synapses revealed the enrichment of DEGs in postsynaptic cells, particularly GABA-A receptor, which plays a key role in the inhibitory function of the CNS through its chloride ion channel

Table 1
Number of probes, genes, and samples of each dataset.

GEO dataset	GPL platform	Number of probes	Number of genes (after processing)	Number of samples (after processing)
Hippocampus tissue				
GSE36980	**GPL6244**	**33,297**	**21,175**	**AD 7, non-AD10**
GSE1297	**GPL96**	**22,283**	**13,631**	**AD 17, non-AD 5**
GSE28146	**GPL570**	**54,675**	**22,172**	**AD 15, non-AD 5**
GSE48350	**GPL570**	**54,675**	**22,172**	**AD 18, non-AD 42**
GSE5281	**GPL570**	**54,675**	**22,172**	**AD 10, non-AD 13**
Entorhinal cortex tissue				
GSE48350	**GPL570**	**54,675**	**22,172**	**AD 13, non-AD 34**
GSE5281	**GPL570**	**54,675**	**22,172**	**AD 9, non-AD 11**

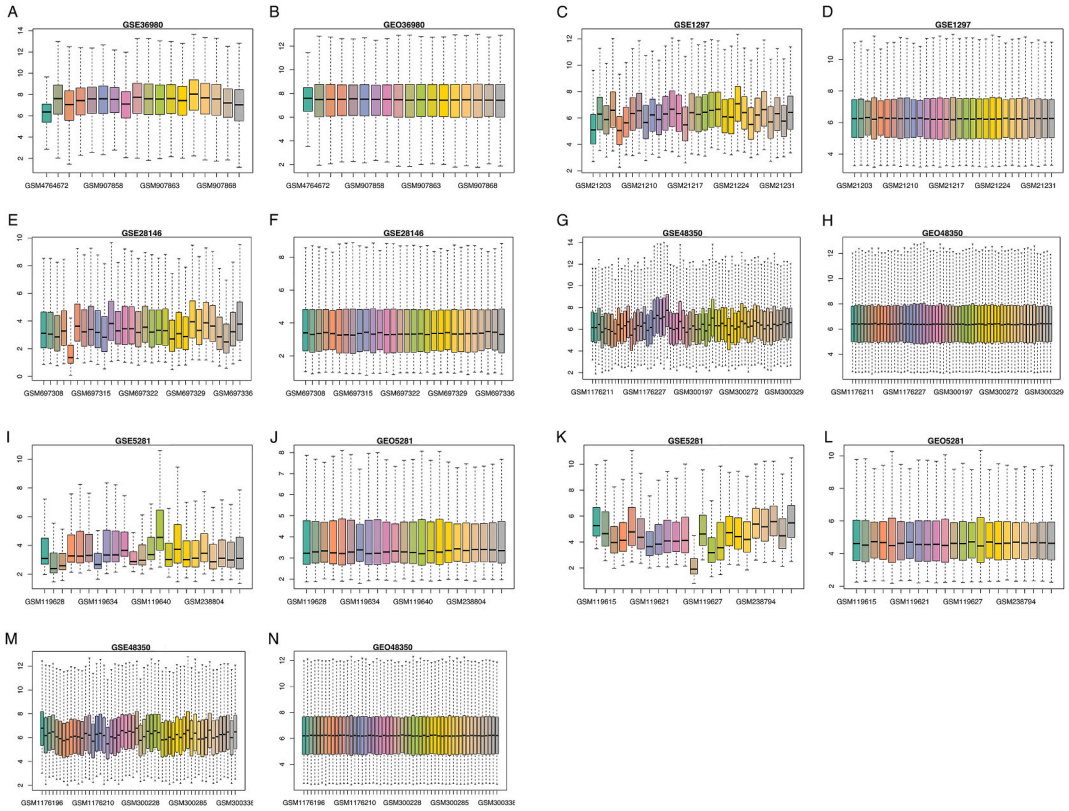

Fig. 2. Box plots of gene expression levels for each dataset in HC (A–J) and EC (K–N). The x-axis represents the name of samples in each dataset. The y-axis represents the log 2 of the gene expression values. The log 2 of raw data for HC tissue are shown in A, C, E, G, and I for datasets GSE36980, GSE1297, GSE28146, GSE48350, and GSE528, respectively. While the log 2 of raw data for EC tissue of GSE5281 and GSE48350 datasets are shown in K and M, respectively. The log 2 of the gene expression values after normalization for HC tissue are shown in B, D, F, H, and J for datasets GSE36980, GSE1297, GSE28146, GSE48350, and GSE5281, respectively. While the log 2 of the gene expression values after normalization for EC tissue of GSE5281 and GSE48350 datasets are shown in L and N, respectively.

(Fig. 6) [36]. Additionally, enrichment in cellular components like "axon terminus" and "dendrite" emphasized the impact of neuronal cytoskeleton in AD. Genes associated with "proton-transporting ATPase activity, rotational mechanism" and "structural constituent of cytoskeleton" suggest significant alterations in cellular energy metabolism and cytoskeletal dynamics were essential for maintaining neuronal structure and function. Together, the presence of shared DEGs between EC and HC highlights the significant dysregulation of synapse, cytoskeleton and mitochondria. This suggests that the disruption of these cellular component's function is central to the AD-related cognitive deficits.

5. Dissecting subregion-specific dysregulation in the entorhinal cortex and hippocampus of Alzheimer's disease

Understanding the specific cellular processes affected by AD in distinct brain regions can provide deeper insights into the disease's pathology. The HC and EC, critical areas for memory and learning, are known to be severely impacted in AD. Following the differential gene expression analysis in five HC datasets, 3766 unique DEGs were identified between non-AD versus AD, and 211 unique DEGs were identified between severe stage versus earlier stages. Whereas the differential gene expression analysis in two EC datasets identified 4745 unique DEGs (Table 2, Supplementary File 3). Among these, several genes were identified as significantly different in more than one dataset, indicating consistent patterns of dysregulation across different studies. The number of up-regulation and down-regulation DEGs of each dataset were visualized using a Venn diagram to illustrate the common DEGs found in more than one dataset. Specifically, we identified 400 down-regulated DEGs and 19 up-regulated DEGs of AD versus non-AD overlapping in HC tissue, while 289 down-regulated DEGs and 187 up-regulated DEGs were overlapping in EC tissue (Fig. 7(A–D), Supplementary File 4). To understand the functional roles of the overlapping DEGs, hereafter called "significant DEGs", we conducted gene ontology enrichment analysis using the DAVID 2024 web-based tool [28].

In cells derived from the HC, the significant DEGs were notably enriched in biological processes related to "spontaneous neurotransmitter secretion", "neurofilament cytoskeleton organization", "synaptic vesicle priming", "gluconeogenesis", and "glycolytic process". Additionally, these DEGs were associated with cellular components such as "synaptic vesicle membrane", "postsynapse" and "dendrite". These findings suggest that neurotransmitter secretion and metabolic process were affected in the HC of AD. Furthermore,

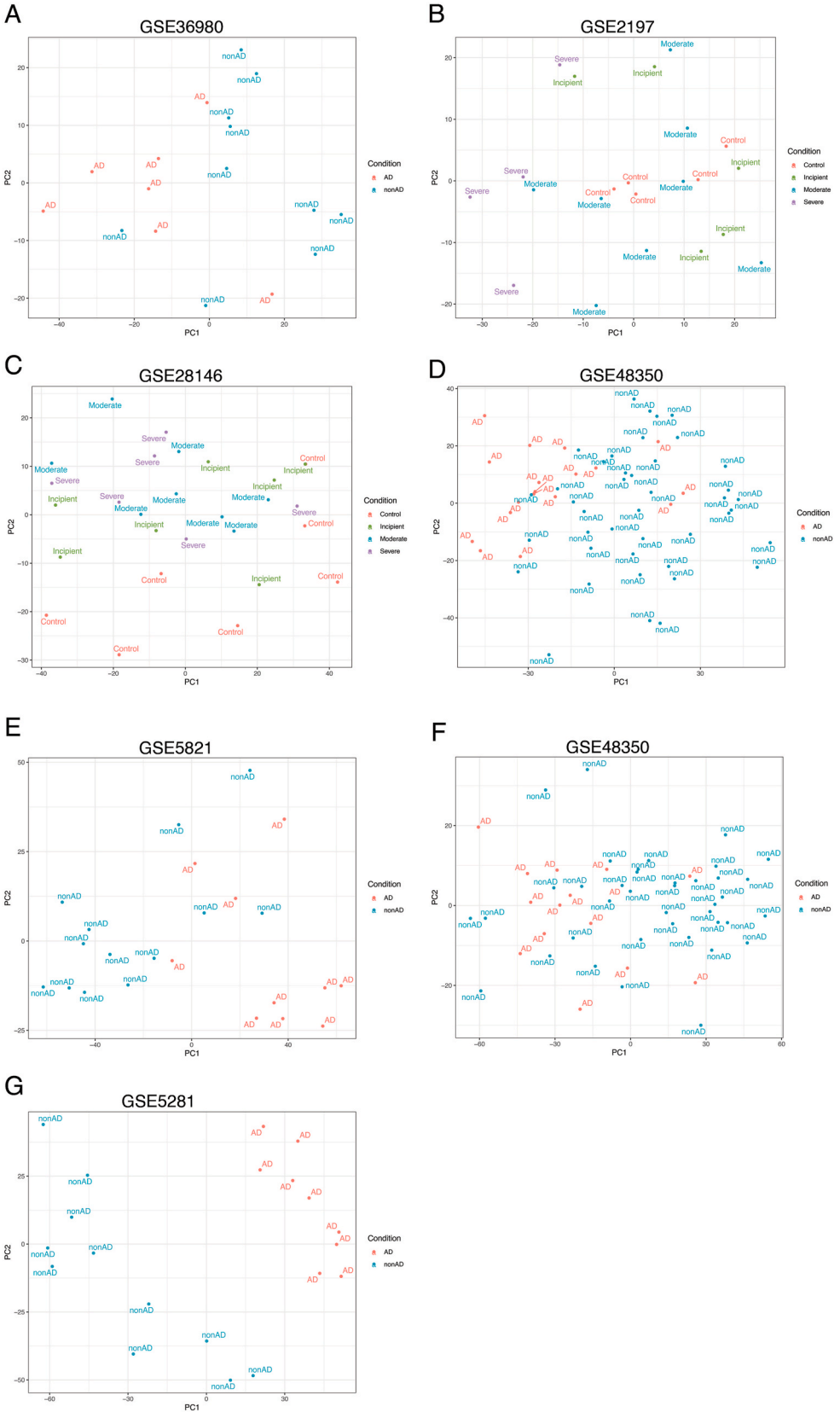

(caption on next page)

Fig. 3. Principal components analysis (PCA) of gene expression in HC and EC tissue. The PCA of gene expression after removing outlier samples are shown for A) GSE36980, B) GSE2197, C) GSE28146, and D) GSE48350, E) GSE5281 from HC tissue. Whereas the PCA of gene expression after removing outlier samples of the EC tissue are shown in F) and G) for the datasets GSE48350 and GSE5281, respectively.

the data suggested the potential dysregulation of mitochondrial processes, particularly those related to proton-transporting ATPase activity and rotational mechanisms. This dysregulation could affect the energy metabolism and mitochondrial function and may contribute to disrupted synaptic activity, bioenergetic process, and neuronal signaling. (Fig. 8(A–D), Supplementary File 5). Notably, eight significant DEGs including *ATP1A3, ATP6V0D1, ATP6V1G2, CRYM, GNG3, MLLT11, PLD3,* and *TAGLN3* were consistently identified across at least three AD versus non-AD and also identified differential difference in severe stage, suggesting their potential shared role in AD pathology. Among these *ATP1A3* and *PLD3* are of particular interest due to their presence in the Human Phenotype Ontology linked to several neuronal degenerations [37]. The identification of these DEGs in multiple datasets underscores its potential role in the pathophysiology of AD which contributed as a promising target for AD therapy.

As previously noted HC samples were obtained from two subregions. GSE1297, GSE28146 and GSE5281 samples collected from the CA1 subregion, whereas GSE48350 and GSE36980 samples were collected from unspecified subregions within the HC. Consequently, the significant DEGs identified in at least GSE1297, GSE28146 and GSE5281 underwent further gene enrichment analysis to investigate the alterations specific to the CA1 subregion. Although differential gene expression analysis of five HC datasets predominantly showed changes in synaptic vesicle dynamics, the analysis of the CA1 subregion also uncovered enrichment in genes involved in processes such as "mitochondrial electron transport from ubiquinol to cytochrome *c*", "aerobic respiration", and "proton transmembrane transport". These genes were linked to mitochondria cellular components, and molecular function of "proton-transporting ATPase activity with a rotational mechanism", and "NADH dehydrogenase (ubiquinone) activity", as well as the KEGG pathway for "oxidative phosphorylation". (Fig. 9(A–D), Supplementary File 5). These results suggest that hypometabolism may initially manifest in the CA1 subregion through mitochondrial dysfunction.

In the EC, gene expression patterns showed alteration in the "gamma-aminobutyric acid signaling pathway", "synaptic transmission, GABAergic", "regulation of postsynaptic membrane potential" and "gluconeogenesis". The gene enrichment analysis of cellular components, molecular functions, and KEGG pathways revealed changes specifically related to "GABAergic synapse", "glutamatergic synapse", "neurotransmitter receptor activity", and "Synaptic vesicle cycle". These alterations in gene expression pattern of these neurotransmitters may be associated with the learning and memory deficit in AD (Fig. 10(A–D), Supplementary File 5). Given that the EC acts as a crucial bridge between the HC and neocortex, facilitating sensory input reception and signal transfer during learning and memory functions, impairment of synaptic vesicle dynamics could contribute to the disruption of communication pathways. EC serves as the primary input and output of HC. They are tightly interconnected with neural pathways. The superficial layer of the EC (layer II) projects the axons to CA1 of HC through the trisynaptic path (TSP) which consists of three main regions. The first synapse occurs between EC layer II to dentate gyrus via the Perforant path. The second synapse from dentate gyrus to CA3 via mossy fibers, and the third synapse from CA3 to CA1 via Schaffer collaterals [38]. This trisynaptic pathway is crucial for the encoding and retrieval of episodic memory. Additionally, CA1 receives direct signals from EC layer III (monosynaptic path; MSP), impacting associative learning and working memory [39,40]. While HC primarily sends axonal projections from CA1 back to EC layers V and VI [38], their interconnections involve both excitatory and inhibitory inputs mediated by neurotransmitters like glutamate, acetylcholine, dopamine, and GABA. Together, the specific regional analysis revealed that the CA1 subregion is particularly vulnerable to bioenergy depletion in AD, while the entire HC experiences impairment in oxidative phosphorylation and bioenergetics. Additionally, alterations in neurotransmitter release observed in the EC are associated with AD clinical symptoms, particularly memory disorders and cognitive decline.

To gain deeper insights into the molecular mechanisms underlying AD, we further analyzed the unique DEGs from these two regions and mapped them to the Alzheimer's disease pathway in KEGG. A total of 54 significant DEGs were identified, distributed across various subcellular compartments, including the cell membrane (6 DEGs), mitochondria (25 DEGs), cytoskeleton (5 DEGs), and cytosol (18 DEGs). They are associated with cell death induced by oxidative stress, ATP depletion, endoplasmic reticulum stress, and calcium signaling. Moreover, these genes show protein kinase activity linked to axonal transport defects, and disruption in neuronal insulin signaling (Fig. 11, green boxes). These findings underscore the vulnerability of mitochondria and the significance of ATP synthesis and oxidative phosphorylation in AD pathology. Overall, the significant DEGs found in both tissues suggest a shared molecular pathway

Table 2
The number of differentially expressed gene in GEO datasets [16].

Tissue	Comparison	GEO dataset	Number of down-regulated genes	Number of up-regulated genes	Number of total DEGs
Entorhinal Cortex (EC)	AD vs non-AD	GSE48350	547	434	981
	AD vs non-AD	GSE5281	2900	1340	4240
Hippocampus (HC)	Severe vs Incipient	GSE1297	294	34	328
	Severe vs Moderate	GSE1297	301	34	335
	Severe vs non-AD	GSE1297	87	22	109
	Severe vs non-AD	GSE28146	8	1	9
	AD vs non-AD	GSE36980	250	25	275
	AD vs non-AD	GSE48350	722	282	1004
	AD vs non-AD	GSE5281	2198	645	2843
Both tissues (EC + HC)			143	8	151

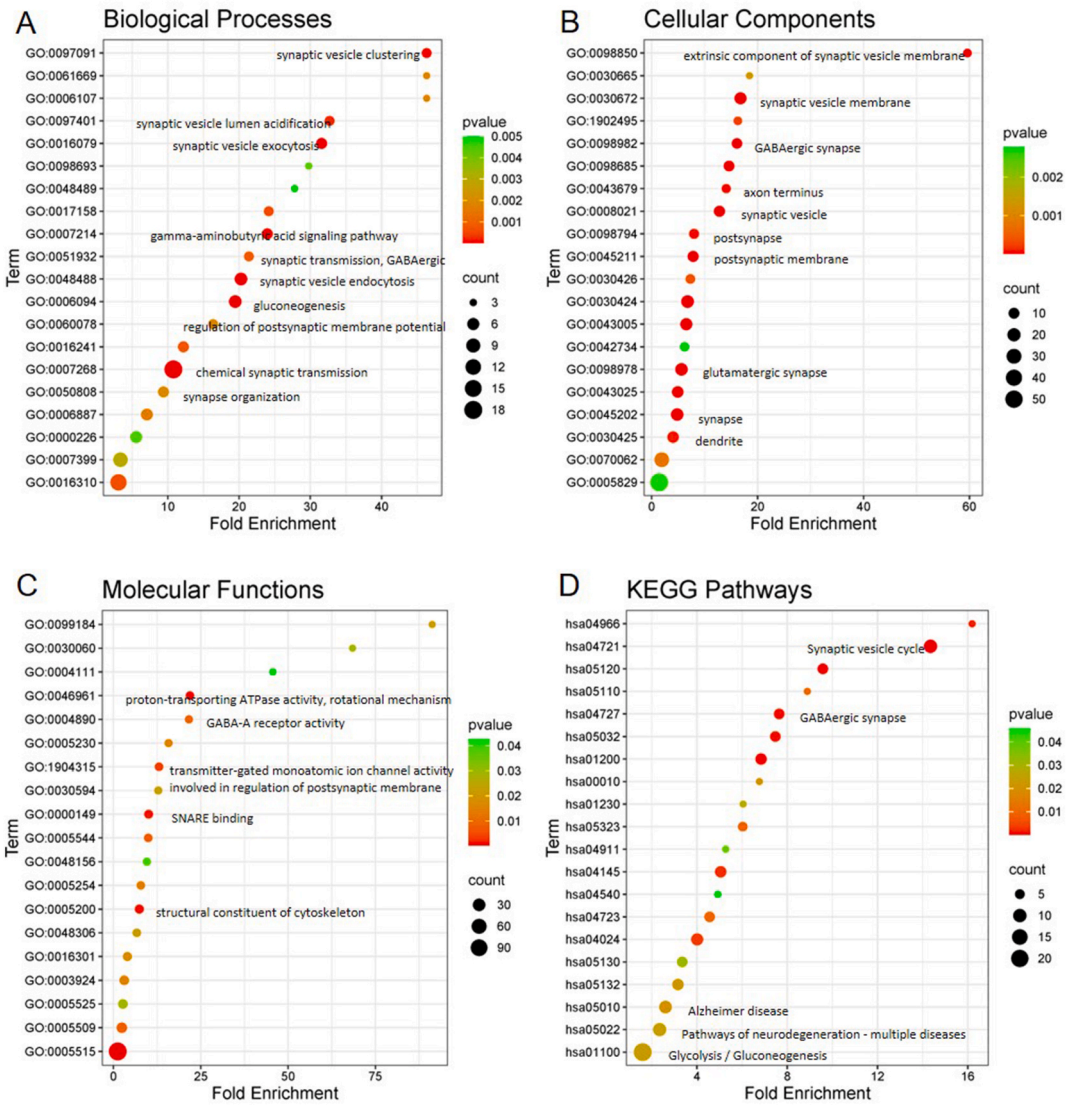

Fig. 4. The functional enrichment analysis bubble diagrams of 151 common DEGs from HC and EC datasets by DAVID. GO categories: A) Biological processes; B) Cellular component; C) Molecular functions; and D) KEGG (Kyoto Encyclopedia of Genes and Genomes) pathway analysis. Modified Fisher Exact p-value less than 0.05. Bubble size represents the number of enriched genes, and bubble color difference represents the significance of target gene enrichment.

involving synaptic signaling, mitochondrial function, and cytoskeletal integrity that were significantly disrupted across the AD brain.

6. Stage-specific transcriptomic alterations in the entorhinal cortex and hippocampus of Alzheimer's

In the analysis of AD stages using dataset GSE1297 and GSE28146, significant DEGs were detected primarily in comparisons involving "severe versus non-AD" (118 DEGs), "severe versus moderate" (335 DEGs), and "severe versus incipient" (328 DEGs), while no significant DEGs were found in "moderate versus non-AD" "moderate versus incipient" and "incipient versus non-AD" comparisons (refer to Table 2). Suggesting that cellular response may occur during early stage and compensate for the gene alteration, while they become more pronounced as the disease progresses.

This study identified significant 61 DEGs across all three comparisons; "severe versus non-AD", "severe versus moderate", and "severe versus incipient" (Fig. 12(A), Supplementary File 5). This suggested potential involvement of these genes in the progression toward the severe stage. Gene enrichment analysis showed that these genes were significantly associated with biological processes of "glycolytic process" and "microtubule cytoskeleton organization" and in the KEGG pathway of "Glycolysis/Gluconeogenesis" (Fig. 12 (B)). Suggesting that hypometabolism was consistently present in the severe stage. Additionally, 24 DEGs were found exclusively in the comparison of "severe versus non-AD" but were absent in "severe versus moderate" and "severe versus incipient" comparisons. These

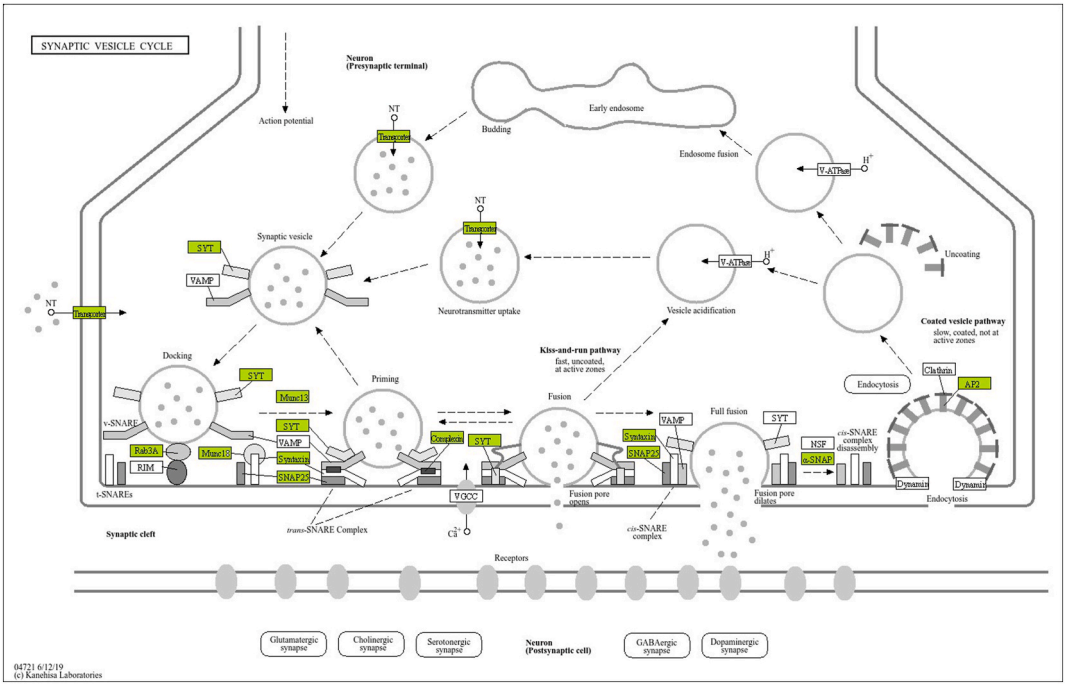

Fig. 5. Synaptic vesicle cycle pathway modified from the KEGG database [29]. The protein marked in green indicated the significant DEGs in the current study.

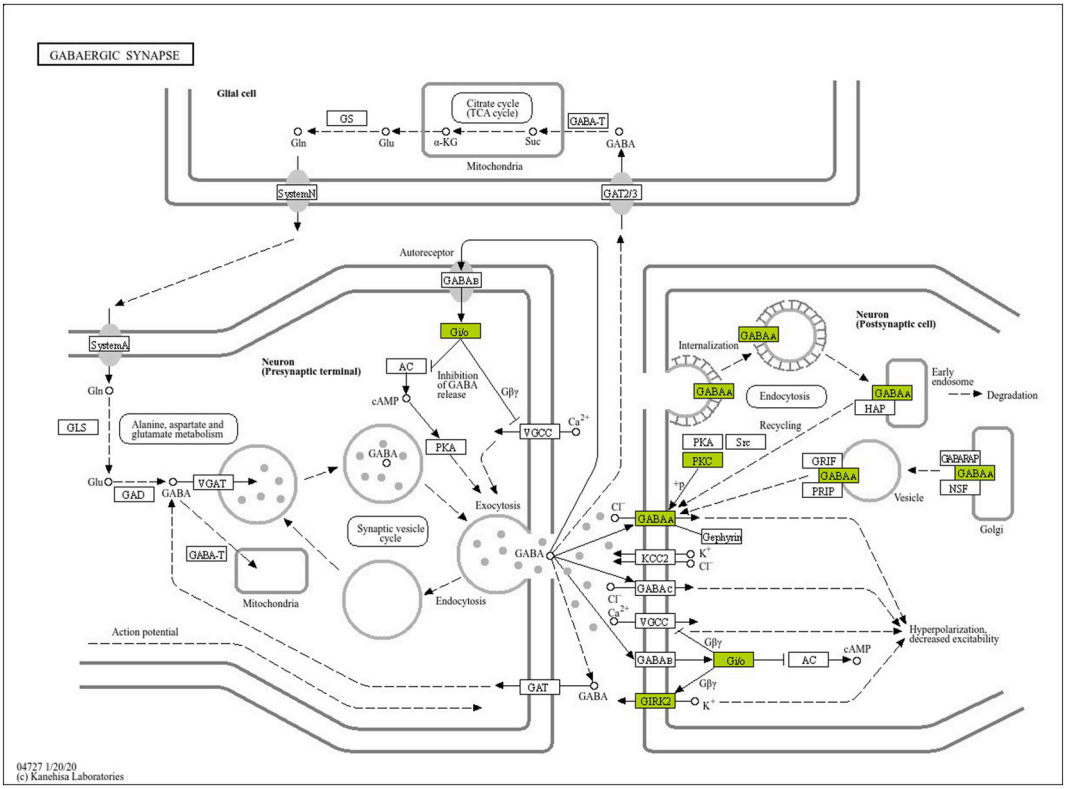

Fig. 6. GABAergic synapse pathway modified from the KEGG database [29]. The protein marked in green indicated the significant DEGs in the current study.

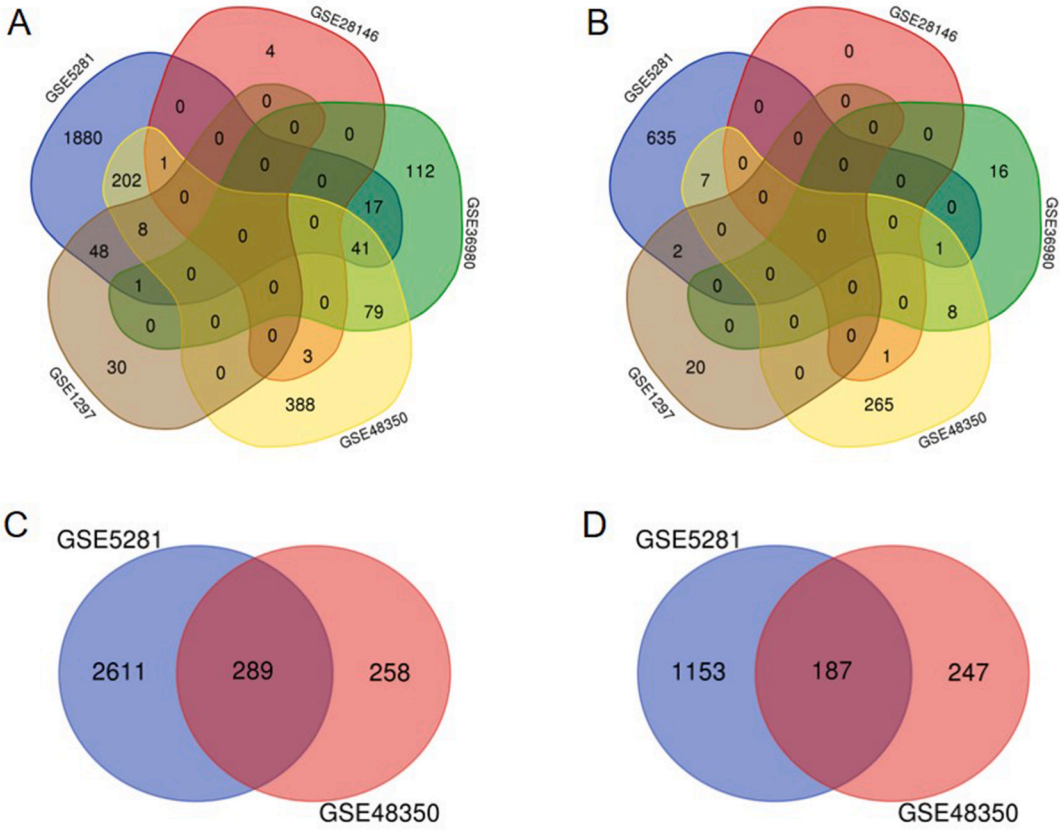

Fig. 7. Venn diagrams show the number of A) up-regulated DEGs and B) down-regulated DEGs of AD versus non-AD in the hippocampus from 5 datasets. C) up-regulated DEGs and D) down-regulated DEGs in the entorhinal cortex from 2 datasets in comparison between AD and non-AD.

genes were enriched in processes such as regulation of transcription, protein stabilization, protein refolding, and p53 binding (Supplementary File 5). These results suggested that transcriptional regulation, particularly through the p53 pathway, may play an important role in the transition from a normal to a diseased state. Together, the stage-specific analysis revealed the significant involvement of metabolic pathways and cytoskeletal organization in the severe stage, while the transcriptional regulation plays a pivotal role in the onset of the disease. However, it's important to note that these conclusions are based on the data of two datasets, GSE1297 and GSE28146, which were derived from similar tissue samples (although they were conducted by different microarray; refer to Table 1). Therefore, this may introduce confounding biases related to the study design and tissue demographic similarities.

7. Protein-protein interaction analysis Reveals ATP synthase subunits as central hub proteins linked to mitochondrial dysfunction and neurotransmitter regulation in AD

To elucidate the underlying mechanisms of AD pathogenesis in the HC and the EC, a PPI analysis was conducted. This study focused on identifying significant gene-encoding proteins and their physical interactions, providing insights into potential therapeutic targets for AD. A total 564 DEGs in HC and 479 DEGs in EC were input into the STRING database, yielded 860 gene-encoding protein data visualized through the Cytoscape/StringApp [30]. The up-regulated genes were represented by yellow circles and down-regulated genes were indicated by blue circles (Fig. 13). The analysis identified 860 nodes and 886 edges with a medium confidence score more than 0.7 and FDR <0.05 (Supplementary file 6).

We identified the top twenty hub genes; *ACTB, GAPDH, CALM3, RPL13A, RPL4, SNAP25, NDUFS3, RPS9, UQCRC1, NDUFV2, UQCRC2, ATP5F1B, RPL8, TUBB, SYT1, NDUFAB1, CYCS, RPL35, RPL6,* and *NDUFB8* that exhibited more than 18 degree of interaction. All of which were down-regulated. Among these, eleven hub genes were classified as non-housekeeping genes. Eight of them; *NDUFS3, UQCRC1, NDUFV2, UQCRC2, ATP5F1B, NDUFAB1, CYCS,* and *NDUFB8* were expressed in mitochondrial while three of them; *CALM3, SNAP25,* and *SYT1* were expressed in synaptic vesicle. Interestingly, eight hub genes expressing in mitochondria mainly associated with electron transport chain complex I (*NDUFS3, NDUFV2, NDUFAB1* and *NDUFB8*) and complex III (*UQCRC1 and UQCRC2*). Suggesting the oxidative phosphorylation may play an important role in dysregulation in HC and EC of AD. In addition to receiving and transferring electrons, these genes involved in generating proton gradient across mitochondrial transmembrane. The proton gradient moves across mitochondrial membrane through F_0 of ATPase or complex V, and consequently rotates F_1ATPase to

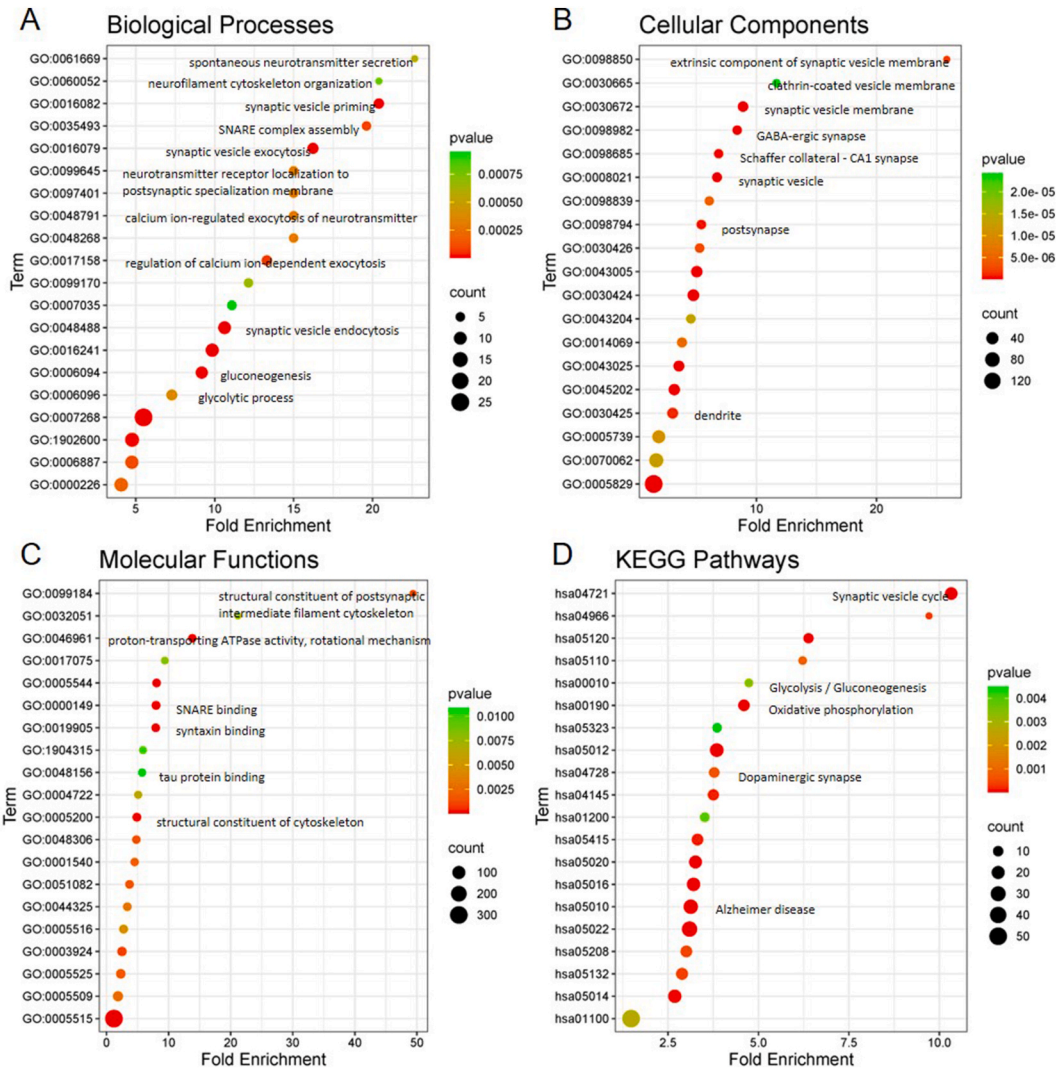

Fig. 8. The functional enrichment analysis bubble diagrams of 419 significant DEGs from four HC datasets by DAVID. GO categories: **A)** Biological processes; **B)** Cellular component; **C)** Molecular functions; and **D)** KEGG (Kyoto Encyclopedia of Genes and Genomes) pathway analysis. Modified Fisher Exact p-value <0.05. Bubble size represents the number of enriched genes, and bubble color difference represents the significance of target gene enrichment.

synthesize ATP. *ATP5F1B* were among genes expressing in mitochondria. It encoded ATP Synthase F1 subunit-beta (ATP5B) which expressed in complex V and involved in ATP synthesis. This mitochondrial dysfunction pointed to the impairment in cellular energy metabolism, which is critical for the physiological function of neurons. The PPI network analysis revealed that *ATP5F1B* interacts with *ATP6V1A, ATP5PF, UQCRC1, ATP6V1B2, ATP5MC3, ATP6V1E1,* and *SLC25A4*, which are enriched in the biological process of proton transmembrane transport. These proteins contribute to generating a proton gradient across membranes, which is essential for ATP production. Notably, hub proteins expressed in synapses predominantly interacted with other proteins within the synaptic vesicle. We also found that mitochondrial proteins were among those interacting with proteins from other subcellular components. Specifically, *ATP5F1B* interacts with *ATP6V1A, ATP6V1G2, ATP6V1B2,* and *ATP6V1E1*, which are involved in synaptic vesicle acidification and neurotransmitter loading. This suggested that key hub proteins may regulate neurotransmitter release by maintaining the proton gradient across the vesicular membrane.

In addition to these top hub genes, we also identified significant genes present in three or more HC datasets and both EC datasets, highlighting their relevance to AD pathology in these regions. These included *GABBR2, UBE2N,* and *TUBB2A* (with 12 degree of interactions); *ATP6V0D1, GPI,* and *GABRG2* (with 10 degree of interactions); and *ATP6V1G2* and *CDK5* (with 8 degree of interactions). Although these genes were not among the top 20 highest hub genes, they rank within the top 100. Their presence in the DEGs of multiple datasets underscored their significance in AD pathology. These genes were enriched in "proton-transporting ATPase activity, rotational mechanism" and "synaptic vesicle lumen acidification". Suggesting that these biological processes may play critical roles in the pathophysiology of AD. Cyclin-dependent kinases 5 (CDK5) has been previously known to control synaptic plasticity through

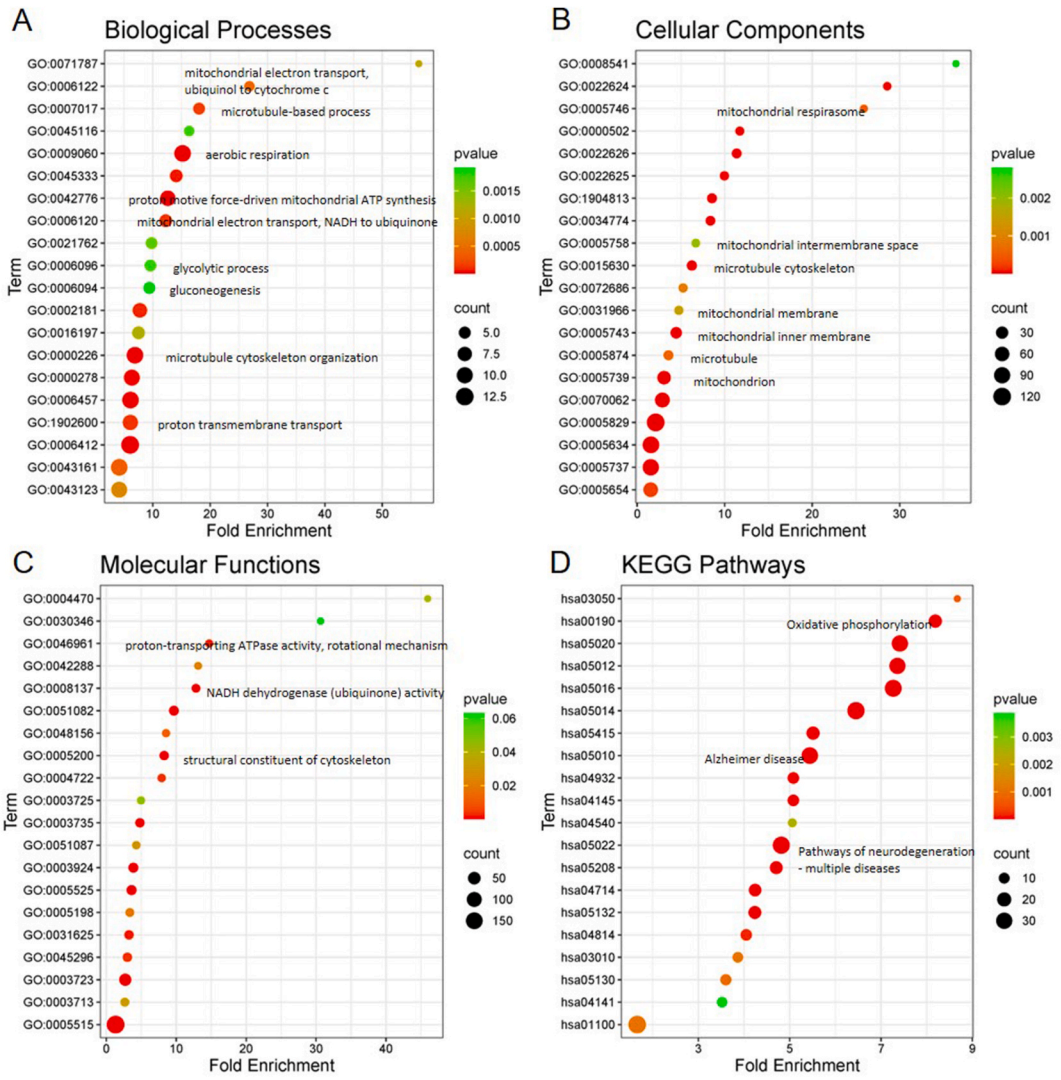

Fig. 9. The functional enrichment analysis bubble diagrams of significant DEGs from three CA1 datasets by DAVID. GO categories: A) Biological processes; B) Cellular component; C) Molecular functions; and D) KEGG (Kyoto Encyclopedia of Genes and Genomes) pathway analysis. Modified Fisher Exact p-value <0.05. Bubble size represents the number of enriched genes, and bubble color difference represents the significance of target gene enrichment.

multiple processes [41,42]. In AD, CDK were reported as a player modulating pathogenesis of AD such as inducing tau-hyperphosphorylation and Aβ accumulation. Furthermore, the involvement of synaptic vesicle-associated genes, particularly those linked to GABA and glutamate signaling, highlights the disruption in neurotransmitter systems. ATP6V0D1 and ATP6V1G2 were relevant to neurotransmitter loading into the synaptic vesicle, thus in down-regulation of theses gene in AD may associated with the neurotransmitter secretion especially glutamate, GABA, acetylcholine and monoamines which required vacuolar H^+-ATPase for their loading into the vesicle.

As previously mention, this study identified the alteration of glutamatergic synapse and GABAergic synapse were enriched in AD samples. The PPI analysis identified two significant genes (*GABRG2* and *GABBR2*) of GABAergic synapse had high degree of interaction. This indicated that GABA neurotransmitters may play a central role in regulating neuronal function of HC and EC neurons. Both genes encoded GABA-A and GABA-B receptors, respectively. They mediated hyperpolarization through the chloride (Cl^-) ion channel (GABA-A receptor) as well as opening potassium (K^+) channels and inhibiting calcium (Ca^{2+}) channels through G-coupled proteins (GABA-B receptor) [36,43]. This neurotransmitter was mainly secreted by inhibitory interneurons. It inhibited neuronal firing and participating in neuronal network modification [43,44]. Such disruptions could interfere synaptic transmission, and resulting in memory and cognitive decline in AD.

The identification of these hub and significant genes highlights the complex nature of AD, where mitochondrial dysfunction and synaptic impairment both contributed to disease progression. The down-regulation of mitochondrial genes involved in oxidative

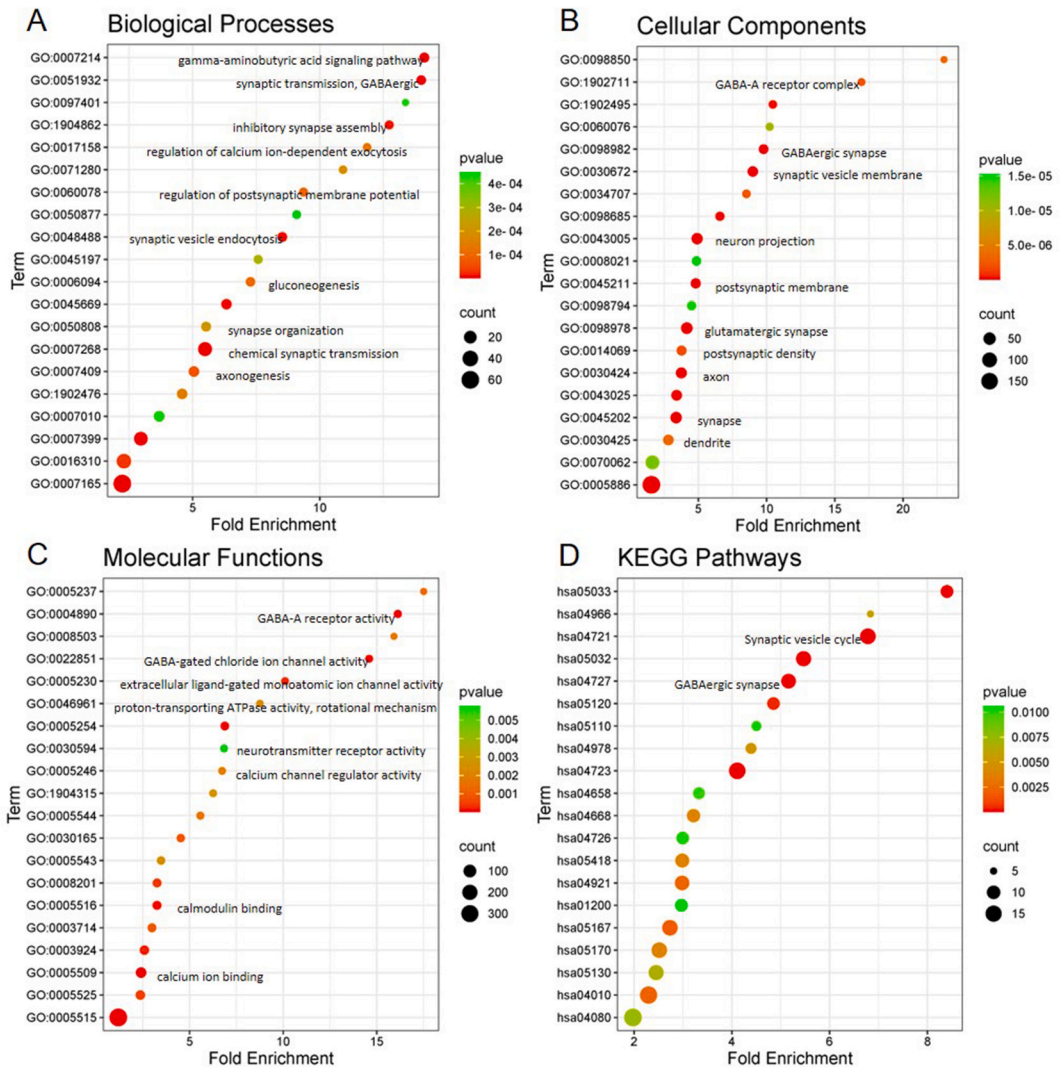

Fig. 10. The functional enrichment analysis bubble diagrams of 476 significant DEGs from two EC datasets by DAVID. GO categories: **A)** Biological processes; **B)** Cellular component; **C)** Molecular functions; and **D)** KEGG (Kyoto Encyclopedia of Genes and Genomes) pathway analysis. Modified Fisher Exact p-value <0.05. Bubble size represents the number of enriched genes, and bubble color difference represents the significance of target gene enrichment.

phosphorylation, alongside disruptions in synaptic vesicle-associated genes, suggests that both energy metabolism and neurotransmitter signaling are vulnerability in AD. Therefore, targeting these pathways could provide therapeutic opportunities to mitigate the effects of the disease.

8. Discussion

Our study delved into the intricate molecular landscape of AD by focusing on the HC and EC, brain regions crucial for memory and learning. AD is one of the most prevalent neurodegenerative disease, contributing to memory decline in the elderly worldwide. Despite its significant impact, the etiology of the disease remains elusive. AD can be categorized into late-onset (sporadic AD) and early-onset (familial AD). Notably, sporadic AD accounts for the majority or about 95 %, while familial AD is relatively rare. Hence, the genome-wide study was conducted to unraveling the disease's etiology [45,46]. However, brain is the organ composed of multiple cell types with distinct functions, a focused transcriptomic analysis of specific brain subregions is essential for a comprehensive understanding of AD pathology.

Previous study has revealed the coherent relationship between cognitive impairment and pathological hallmarks including Aβ plaques and NFTs [47]. These hallmarks tend to be abundant the region likes CA1 of the HC, the EC and the neocortex [48–50]. EC and HC situate in the medial temporal lobe which play pivotal role in learning and memory process. Consequently, the observed atrophy of these regions aligns with the memory decline seen in AD patients [51,52]. Therefore, our study focused on these critical brain areas by

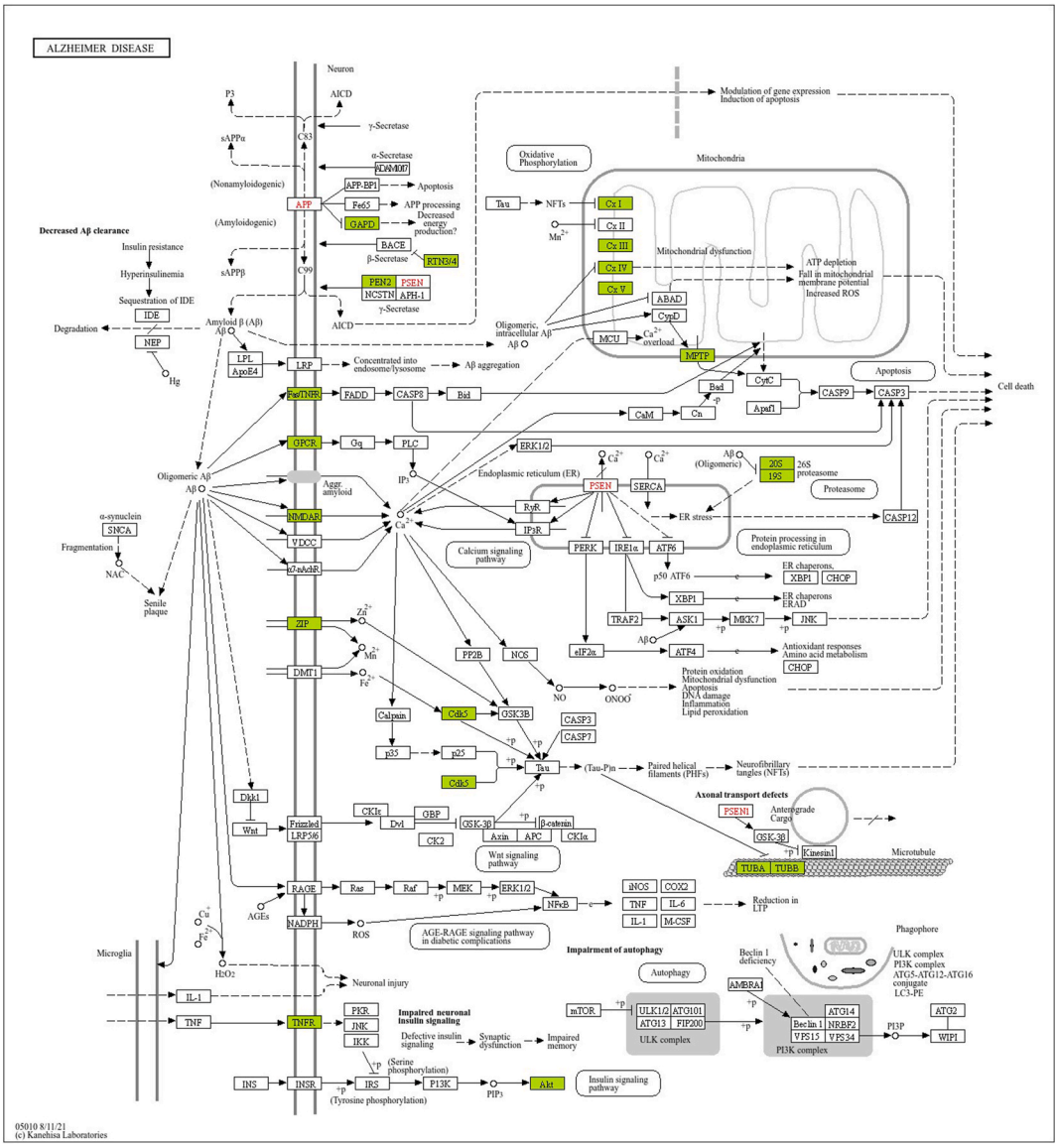

Fig. 11. Alzheimer's disease pathway modified from the KEGG database [29]. The protein marked in green indicated the significant DEGs in the current study.

analyzing transcriptomic data from public repositories. In this study, we retrieved five datasets including GSE36980, GSE1297, GSE28146, GSE48350, and GSE5281 dataset, which conducted microarray in the EC and the HC tissues. Through our investigation, we identified 564 significantly differentially expressed genes in HC and 479 genes in EC presenting in at least two of these datasets. The analysis of these DEGs revealed that biological processes including synaptic vesicle cycle, neurotransmitter secretion (specifically GABA and glutamate), mitochondrial electron transport, and bioenergetics, were significantly altered in AD samples compared to non-AD samples. To validate our findings, we compared them with results from the RNA sequencing dataset GSE173955 [53], which conducted the differential gene expression between AD versus non-AD in human HC. This comparison demonstrated consistency with our findings, reinforcing the reliability of our results across different platforms.

The analysis in HC identified *ATP1A3* as a DEG in several GSE datasets including GSE36980, GSE48350, and GSE5281, comparing AD versus non-AD sample. In all of these comparisons, ATP1A3 consistently down-regulated in AD. Additionally, in the stage specific analysis of the GSE1297 dataset, significant down-regulation of *ATP1A3* was also observed in the severe stage of AD compared to incipient and moderate stages. *ATP1A3,* encoded Na+/K + ATPase alpha 3 subunit, is critical for maintaining sodium (Na^+) and potassium (K^+) ions across neuronal membrane. Although the association of *ATP1A3* and AD remained to be underexplored, its involvement in other neurodegenerative disorders provides evidence of its potential role in the cognitive decline [54,55]. Furthermore, this study also identified the down-regulation of *PLD3* genes in four transcriptomic analysis including GSE1297, GSE36980, GSE48350,

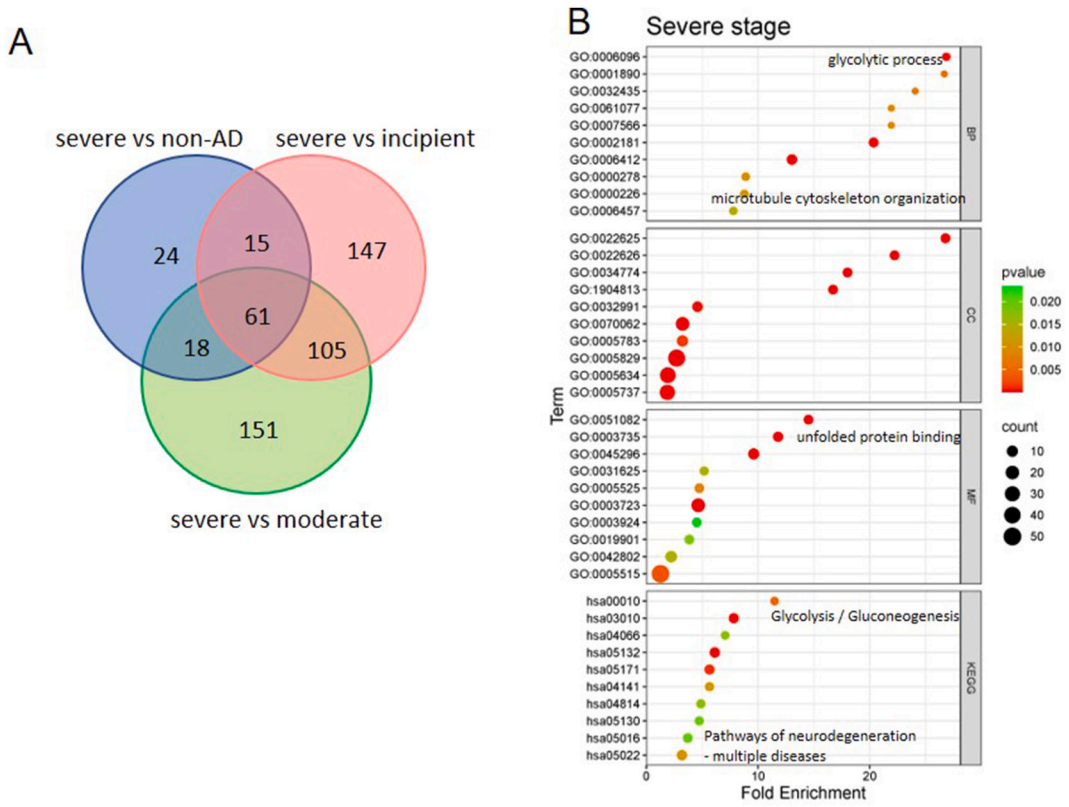

Fig. 12. A) Venn diagrams show number of up-regulated and down-regulate DEGs from GSE1297 and GSE 28146 datasets in comparison among severe stages versus others. B) Bubble diagrams of top 10 functional enrichment analysis of 61 DEGs. GO categories: BP biological processes; CC cellular component; MM molecular functions; KEGG Kyoto Encyclopedia of Genes and Genomes. Modified Fisher Exact p-value less than 0.05. Bubble size represents the number of enriched genes, and bubble color difference represents the significance of target gene enrichment.

and GSE5281. This finding aligns with previous research showing that the rare coding variants of lysosomal protein PLD3 are risk factor for AD which contributed to amyloid plaque accumulation and cognitive impairment [56–58]. Previous studies have shown that hypometabolism in specific brain areas is associated with clinical symptoms of AD [59–61] and may even precede the onset of memory impairment [59]. Impaired ATP-dependent processes, such as disrupted Na^+/K^+ ATPase activity, can lead to ionic imbalances that exacerbate neuronal dysfunction and lead to cognitive deficits in AD. Additionally, the mitochondrial energy metabolism impairment has been observed in other brain regions affected by AD, including the posterior cingulate cortex and the middle temporal gyrus [61]. A study using a transgenic rat model further revealed impaired glucose uptake in the EC and HC [62]. These findings suggest a strong correlation between low brain energy metabolism and impaired brain functions.

Alongside with hypometabolism, oxidative stress is a common feature observed in several neurodegenerative diseases, including AD. Among respiratory chain abnormality, deficiency in complex I is frequently observed [63,64]. This deficiency inhibited of NADH dehydrogenase, leading to excessive accumulation of Reactive Oxygen Species (ROS), subsequently affecting the function of mitochondrial complexes III, IV, and V [65]. Previous studies have demonstrated that Aβ accumulation can exacerbate this dysfunction, particularly affecting complexes I and IV, leading to extreme ROS production and a subsequent increase oxidative stress and decrease neuronal ATP levels [66]. The accumulation of ROS, in turn, associated with cytoskeletal impairment, tau phosphorylation, and increased Aβ production [67]. Furthermore, neurotoxic oligomeric Aβ disrupted Ca^{2+} homeostasis, affecting synaptic vesicle trafficking and cytoskeletal organization. Oxidative stress has also been linked with tau hyperphosphorylation, contributing to the formation of NFTs [68,69].

In this present study, the PPI analysis identified mitochondrial complexes I, III, and V as the locations of top twenty central hub proteins. Additionally, the comparison among three AD stages revealed that common DEGs in the severe stage were associated with bioenergetic process. These findings suggest that the dysregulation of energy metabolism was commonly found in the late stage of the disease, subsequently impairing neuron functions in the EC and HC. Moreover, the identification of DEGs related to transcriptional regulation through p53-mediated pathways may play a pivotal role in the transition from a healthy to a diseased state. The p53 pathway, previously identified dysregulated in mild cognitive impairment (MCI) and AD and induced neuronal apoptosis [70]. This process may be involved in the early cellular responses to stress in AD, potentially acting as a regulator of gene expression that drives disease onset. Indicating that in addition to targeting bioenergetic deficits, therapeutic strategies focused on modulating p53 activity could help mitigate the early transcriptional dysregulation that contributes to AD progression.

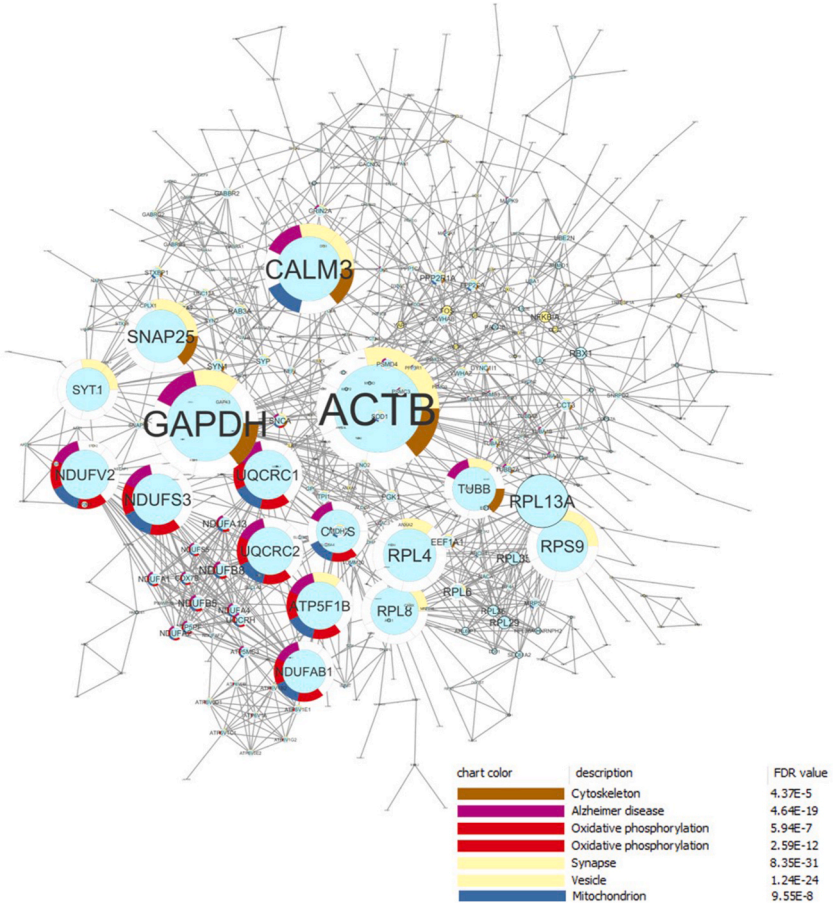

Fig. 13. PPI subnetwork of DEGs from HC and EC tissue. Nodes represent genes. Edges represent the interactions between genes from the String database. The network shows a largest subnetwork. The color ring of each node highlighted the enrichment analysis of cellular component and key pathways including Oxidative phosphorylation and AD pathway.

Our PPI analysis identified mitochondrial proteins as central hub proteins. Among these, NADH:Ubiquinone Oxidoreductase, Ubiquinol-Cytochrome C Reductase, and ATP Synthase, were involved in mitochondrial oxidative phosphorylation, suggesting impaired energy metabolism in AD. In particular, *ATP5F1B* was interested. It encoded ATP Synthase F1 subunit-beta and were down-regulation in both regions. This finding concurred with previous studies showing that ATP5B protein was repressed in AD brain samples, as analyzed by iTRAQ proteomic methods [71], and there was a reduction in ATP synthase enzyme activity in AD [71–73]. Additionally, Aβ exposure has been shown to suppress ATP5B expression in the HC [71,74]. While the glycosylation of alpha subunit of ATP synthase acted as an extracellular domain for Aβ binding site and inhibited ATPase activity [71,75]. Suggesting that that reduction of ATP synthesis may associated with the accumulation of Aβ. The association between the progression of AD and mitochondrial impairment has been emphasized in numerous reviews [51,65,76]. Notably, the impairment of ATP synthase has been previously implicated in various neurodegenerative diseases, including AD [61,77,78]. Suggesting that ATP synthase subunit protein may play a pivotal role in the clinical characteristics observed in the HC and EC. Furthermore, the synaptic vesicle-associated genes like *SNAP25* and *SYT1* highlighted neurotransmitter dysregulation, particularly in GABAergic signaling. The high degree of interaction observed between *GABRG2* and *GABBR2* suggested that GABA neurotransmitters play an important role in regulating the neuronal network in the HC and EC. GABAergic signaling is crucial for maintaining the balance between excitation and inhibition within these regions. In the HC, GABA is primarily released from interneurons, which modulate the activity of pyramidal neurons, thus influencing processes like memory encoding and retrieval. In the EC, GABAergic projections help to regulate the integration of sensory information and the formation of associative memories. Therefore, the dysregulation of GABA signaling in these regions has been linked to cognitive deficits in AD.

In addition, the CDK5 was among significant genes with high interaction. Enhancing CDK5 activity may associated with cognitive decline and learning impairment in AD, which was believed to be associated with the binding of CDK5 with p25 [79,80]. Studies in animal model revealed that CDK5 knockout mice increased synaptic plasticity and enhanced hippocampal long-term potentiation (LTP) [41]. In addition, the injection of short hairpin RNA (CDK5 shRNA-miR) into AD mice hippocampi resulted in the recovery of LTP [42]. Although several previous studies revealed the hyperactivity of CDK5 in AD models and postmortem tissues, the expression

of *CDK5* gene assessed by real-time-PCR [81] and RNA sequencing technique [53] in AD postmortem tissues revealed the down-regulation of this gene. Similar to what we observed in microarray datasets, *CDK5* genes presented as down-regulated DEGs in GSE36980, GSE48350, and GSE5281 analysis. The contradiction between CDK activity and gene expression could be explained that CDK5 activity may be regulated by its activators such as p35 or p25 (the cleavage product of p35), or the compensatory mechanism in mouse model. Therefore, targeting CDK5 as a therapeutic target should be strictly regulated and require further study to understand the role of CDK5 in AD.

In this study, our focus was on investigating gene expression patterns within HC and EC, both well-established regions involved in memory and learning processes. The connection between CA1 region of HC and EC is facilitated by synaptic pathways including monosynaptic pathway (MSP) and trisynaptic pathway (TSP). The MSP primarily contributes to the formation and retrieval of associative learning and spatial memory processes, while TSP is associated with the formation and retrieval of episodic memory. Our gene enrichment analysis in CA1 region revealed significant differential gene expression in genes related to gluconeogenesis, synaptic endocytosis and ATP synthesis couple proton transport. Similarly, the enrichment analysis in EC showed the difference in synaptic endocytosis, exocytosis, and ATP synthesis couple proton transport. These finding suggested the reduction in ATP synthase subunits protein expression in both regions, with gluconeogenesis primarily reduced in the CA1 region. Furthermore, the dysfunction in synaptic endocytosis and exocytosis was observed in EC region. These findings underscore the role of the EC as a pivotal neural circuit between HC and the neocortex, mediating functions in associative learning, spatial memory, and episodic memory processes (Fig. 14).

Given that clinical diagnosis indicates AD patients are primarily affected in episodic memory, the connection between the EC and HC through the MSP and TSP pathway should be considered. Together with previous observations implicating hypometabolism in the early stages of AD [76] and our analysis implicating dysregulation of synaptic dynamics and membrane potential in severe stages, we propose that mitochondrial impairment, particularly involving bioenergetic deficits in the CA1 region, occurs early in disease progression. This mitochondrial dysfunction likely continues, resulting in the dysregulation of oxidative phosphorylation and the electron transport chain in the HC. Consequently, ATP synthesis is disrupted, affecting all ATP-dependent pathways, such as neurotransmitter release.

In recent decades, research has increasingly focused on the role of mitochondria in AD, with several mitochondrial-targeted therapies being investigated [82]. Examples include those targeting oxidative stress, such as Ginkgo biloba [83], N-acetylcysteine (NAC) [84], SkQ1 and MitoQ [85,86], as well as bioenergetic therapies like SS31 [87] and Pioglitazone [88]. Although some of these therapies have shown promising results in the early phase trials, none have definitively passed clinical trials for AD. Ongoing research is essential to determine their efficacy and safety as a therapeutic target in AD. While the study of human samples inherits numerous

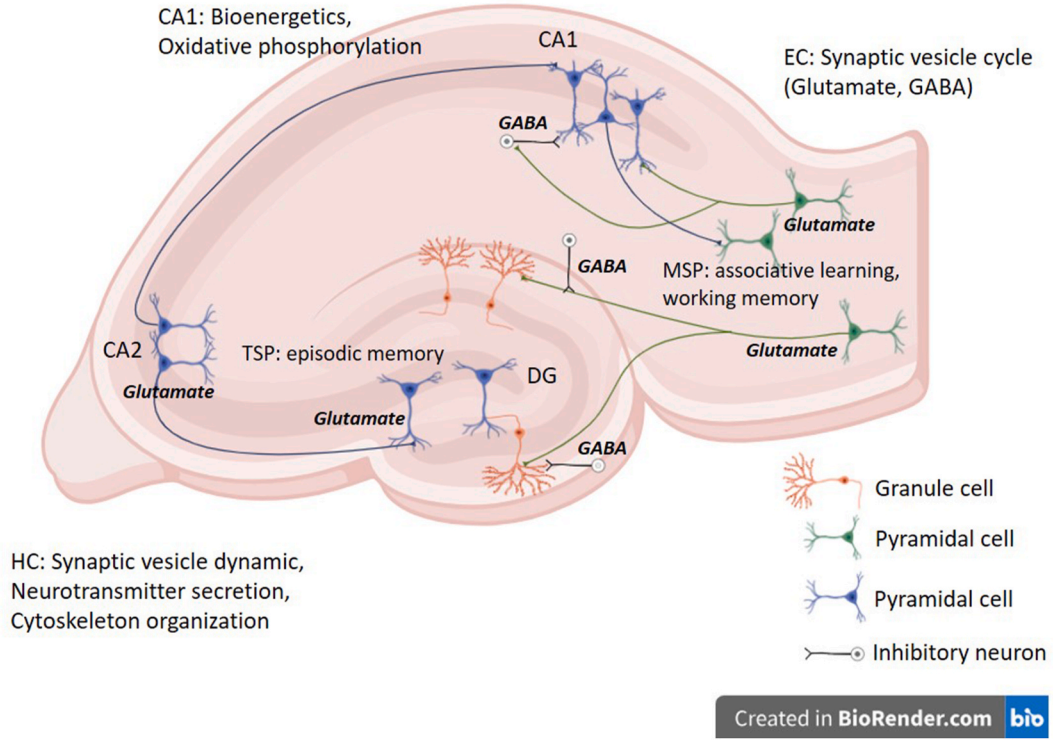

Fig. 14. Schematic of brain subregions supporting the role of HC and EC in learning and memory, and predicted biological process involving cognitive decline in AD. This image was generated by BioRender software [89].

variables, including the challenge of controlling for disease background, comorbidity, potential treatment effects, and lifestyle factors when compared to animal models, we have found that conducting a cross-transcriptomic analysis of multiple microarray data could help mitigate these challenges and provide a more comprehensive understanding of AD.

9. Conclusion

Our findings highlight significant transcriptomic alterations in the HC and EC. We identified the dysregulation in bioenergetic processes, synaptic dynamics especially GABAergic signaling in AD tissues. The consistent down-regulation of key genes, including *ATP5F1B* and *ATP1A3*, underscores the impact of hypometabolism and ionic dysregulation on cognitive decline. These results emphasize the potential importance of targeting mitochondrial functions for AD therapy, particularly for mitigating cognitive impairment associated with the hippocampal and the entorhinal cortex degeneration. Since our analysis focused solely on specific brain regions, future investigations should also explore transcriptomic changes in other brain regions implicated in AD pathology, and consider gender-specific analyses to provide further insights into the disease mechanisms.

CRediT authorship contribution statement

Pajaree Sonsungsan: Visualization, Software. **Supatha Aimauthon:** Writing – original draft, Visualization, Investigation, Formal analysis. **Nattawet Sriwichai:** Visualization, Software, Formal analysis. **Poommaree Namchaiw:** Writing – review & editing, Writing – original draft, Validation, Supervision, Investigation, Funding acquisition, Conceptualization.

Ethics approval and consent to participate

Not applicable.

Availability of data and materials

Five microarray datasets were retrieved from the Gene Expression Omnibus (GEO) public database: https://www.ncbi.nlm.nih.gov/geo/under GSE accession: GSE36980, GSE1297, GSE28146, GSE48350, and GSE5281.

All data generated or analyzed during this study are included in this published article [and its supplementary information files].

Funding

This work was supported by Overseas Research Grants 2021 from Asahi Glass foundation.

PN was supported by Thailand Science Research and Innovation through the Basic Research Fund: Fiscal year 2024 (project number FRB670016/0164).

Declaration of competing interest

The authors declare the following financial interests/personal relationships which may be considered as potential competing interests:

Poommaree Namchaiw reports financial support was provided by Asahi Glass Foundation. Poommaree Namchaiw reports financial support was provided by Thailand Science Research and Innovation. We confirm that there are no personal or professional relationships, affiliations, memberships, or other non-financial interests that could bias our work or the publication of the manuscript. We affirm that there are no intellectual interests that might affect the research or interpretation presented in the manuscript. Our contributions are based solely on scientific merit and professional integrity. We hereby provide this declaration of no conflict of interest in accordance with the ethical standards of scientific publishing, ensuring transparency and integrity in the dissemination of research findings. If there are other authors, they declare that they have no known competing financial interests or personal relationships that could have appeared to influence the work reported in this paper.

Acknowledgements

PS and SA would like to thank PN Lab members for the support throughout the study.

Appendix A. Supplementary data

Supplementary data to this article can be found online at https://doi.org/10.1016/j.heliyon.2024.e39378.

References

[1] G.D.F. Collaborators, Estimation of the global prevalence of dementia in 2019 and forecasted prevalence in 2050: an analysis for the Global Burden of Disease Study 2019, Lancet Public Health 7 (2) (2022) e105–e125.
[2] Alzheimer's Disease Facts and Figures. LID - 10.1002/alz.12068 [doi], 2020, pp. 1552–5279 (Electronic)).
[3] R.C. Barber, The genetics of Alzheimer's disease, Scientifica 2012 (2012) 246210.
[4] J. Cummings, et al., Alzheimer's disease drug development pipeline: 2023, Alzheimer's Dementia: Translational Research & Clinical Interventions 9 (2) (2023) e12385.
[5] LK. Huang, YC. Kuan, HW. Lin, et al., Clinical trials of new drugs for Alzheimer disease: a 2020–2023 update, J. Biomed. Sci. 30 (2023) 1–19. https://doi.org/10.1186/s12929-023-00976-6.
[6] J.R. Pavoni S, F. Nassor, A.-C. Guyot, S. Cottin, J. Rontard, et al., Small-molecule induction of Aβ-42 peptide production in human cerebral organoids to model Alzheimer's disease associated phenotypes 13 (2018) 1–15.
[7] J.a.B. Bamburg, Gs, Cytoskeletal pathologies of Alzheimer disease, Cell Motil Cytoskeleton 66 (8) (2009) 635–649.
[8] Q.a.T.P. Cai, Mitochondrial aspects of synaptic dysfunction in Alzheimer's disease, J Alzheimers Dis 57 (4) (2017) 1087–1103.
[9] H. Braak, E. Braak, Neuropathological stageing of Alzheimer-related changes, Acta Neuropathol. 82 (4) (1991) 239–259.
[10] R.H. Swerdlow, J.M. Burns, S.M. Khan, The Alzheimer's disease mitochondrial cascade hypothesis: progress and perspectives, Biochim. Biophys. Acta (BBA) - Mol. Basis Dis. 1842 (8) (2014) 1219–1231.
[11] V.L. Villemagne, et al., Amyloid β deposition, neurodegeneration, and cognitive decline in sporadic Alzheimer's disease: a prospective cohort study, Lancet Neurol. 12 (4) (2013) 357–367.
[12] A.T. Du, et al., Magnetic resonance imaging of the entorhinal cortex and hippocampus in mild cognitive impairment and Alzheimer's disease, J. Neurol. Neurosurg. Psychiatr. 71 (4) (2001) 441–447.
[13] I.M. McDonough, et al., Young adults with a parent with dementia show early abnormalities in brain activity and brain volume in the Hippocampus: a matched case-control study, Brain Sci. 12 (4) (2022) 496.
[14] O.J. Olajide, M.E. Suvanto, C.A. Chapman, Molecular mechanisms of neurodegeneration in the entorhinal cortex that underlie its selective vulnerability during the pathogenesis of Alzheimer's disease, Biol Open 10 (1) (2021).
[15] Z. Fang, Jeffrey Martin, Wang, Zhong, Statistical methods for identifying differentially expressed genes in RNA-Seq experiments, Cell Biosci. 2 (1) (2012) 26.
[16] R. Edgar, M. Domrachev, A.E. Lash, Gene Expression Omnibus: NCBI gene expression and hybridization array data repository, Nucleic Acids Res. 30 (1) (2002) 207–210.
[17] Series GSE36980. National Center for Biotechnology Information (NCBI).
[18] Series GSE1297. National Center for Biotechnology Information (NCBI).
[19] Series GSE28146. National Center for Biotechnology Information (NCBI).
[20] Series GSE48350. National Center for Biotechnology Information (NCBI).
[21] Series GSE5281. National Center for Biotechnology Information (NCBI).
[22] Davis, S. and P.S. Meltzer,GEOquery: a Bridge between the Gene Expression Omnibus (GEO) and BioConductor. (1367-4811 (Electronic)).
[23] Gautier, L., et al. affy–analysis of Affymetrix GeneChip Data at the Probe Level. (1367-4803 (Print)).
[24] Irizarry, R.A., et al. Exploration, Normalization, and Summaries of High Density Oligonucleotide Array Probe Level Data. (1465-4644 (Print)).
[25] Langfelder, P. and S. Horvath,WGCNA: an R Package for Weighted Correlation Network Analysis. (1471-2105 (Electronic)).
[26] B. Venables, B. Ripley, Modern Applied Statistics with S, 2002.
[27] Ritchie, M.E., et al.,Limma Powers Differential Expression Analyses for RNA-Sequencing and Microarray Studies. (1362-4962 (Electronic)).
[28] Sherman, B.T., et al., DAVID: a web server for functional enrichment analysis and functional annotation of gene lists (2021 Update). (1362-4962(Electronic)).
[29] Kanehisa, M., et al., KEGG as a Reference Resource for Gene and Protein Annotation(1362-4962 (Electronic)).
[30] Doncheva, N.A.-O., et al.Cytoscape StringApp: Network Analysis and Visualization of Proteomics Data. (1535-3907 (Electronic)).
[31] Szklarczyk, D., et al.,The STRING Database in 2023: Protein-Protein Association Networks and Functional Enrichment Analyses for Any Sequenced Genome of Interest. (1362-4962 (Electronic)).
[32] Control 1039, National Center for Biotechnology Information (NCBI), 2004.
[33] J.C. Augustinack, A.J.W. van der kouwe, Chapter 69 - postmortem imaging and neuropathologic correlations, in: J.C. Masdeu, R.G. González (Eds.), Handbook of Clinical Neurology, Elsevier, 2016, pp. 1321–1339.
[34] Igarashi, K.M. Entorhinal Cortex Dysfunction in Alzheimer's Disease. (1878-108X (Electronic)).
[35] Y. Mu, F.H. Gage, Adult hippocampal neurogenesis and its role in Alzheimer's disease, Mol. Neurodegener. 6 (2011) 75–85.
[36] Ghit, A.A.-O., et al. GABA(A) receptors: structure, function, pharmacology, And Related Disorders. (2090-5920 (Electronic)).
[37] Robinson, P.N., et al.,The Human Phenotype Ontology: a Tool for Annotating and Analyzing Human Hereditary Disease. (1537-6605 (Electronic)).
[38] M.P. Witter, et al., Architecture of the entorhinal cortex A review of entorhinal anatomy in rodents with some comparative notes, Front. Syst. Neurosci. 11 (2017).
[39] C. Grienberger, J.C. Magee, Entorhinal cortex directs learning-related changes in CA1 representations, Nature 611 (2022) 554–562. https://doi.org/10.1038/s41586-022-05378-6.
[40] Kitamura, T., C.J. Macdonald, and S. Tonegawa,Entorhinal-hippocampal Neuronal Circuits Bridge Temporally Discontiguous Events. (1549-5485 (Electronic)).
[41] A.H. Hawasli, et al., Cyclin-dependent kinase 5 governs learning and synaptic plasticity via control of NMDAR degradation, Nat. Neurosci. 10 (7) (2007) 880–886.
[42] Posada-Duque, R.A., et al. CDK5 Downregulation Enhances Synaptic Plasticity. (1420-9071 (Electronic)).
[43] Scanziani, M. GABA Spillover Activates Postsynaptic GABA(B) Receptors to Control Rhythmic Hippocampal Activity. (896-6273 (Print)).
[44] Tzilivaki, A., et al.,Hippocampal GABAergic Interneurons and Memory. (1097-4199 (Electronic)).
[45] R.T. Dietmar, et al., Phases of Aβ-deposition in the human brain and its relevance for the development of AD, Neurology 58 (12) (2002) 1791.
[46] D. Furcila, et al., Subregional density of neurons, neurofibrillary tangles and amyloid plaques in the Hippocampus of patients with Alzheimer's disease, Front. Neuroanat. 13 (2019).
[47] S.E. Arnold, et al., The topographical and neuroanatomical distribution of neurofibrillary tangles and neuritic plaques in the cerebral cortex of patients with Alzheimer's disease, Cerebr. Cortex 1 (1) (1991) 103–116.
[48] Adav, S.S., J.E. Park, and S.A.-O. Sze, Quantitative Profiling Brain Proteomes Revealed Mitochondrial Dysfunction in Alzheimer's Disease. (1756-6606 (Electronic)).
[49] L. deToledo-Morrell, T.R. Stoub, C. Wang, Hippocampal atrophy and disconnection in incipient and mild Alzheimer's disease, in: H.E. Scharfman (Ed.), Progress in Brain Research, Elsevier, 2007, pp. 741–823.
[50] Du, A.T., et al.,Higher Atrophy Rate of Entorhinal Cortex than hippocampus in AD. (1526-632X (Electronic)).
[51] B. Ebanks, T.L. Ingram, L. Chakrabarti, ATP synthase and Alzheimer's disease: putting a spin on the mitochondrial hypothesis, Aging (Albany NY) 12 (16) (2020) 16647–16662.
[52] Terni, B., et al., Mitochondrial ATP-synthase in the entorhinal cortex is a target of oxidative stress at stages I/II of Alzheimer's Disease Pathology. (1750-3639 (Electronic)).
[53] *GSE173955*. National Center for Biotechnology Information (NCBI).
[54] X. Zhang, W. Lee, J.-S. Bian, Recent advances in the study of Na+/K+-ATPase in neurodegenerative diseases, Cells 11 (2022), https://doi.org/10.3390/cells11244075.
[55] P.A. Salles, et al., ATP1A3-Related disorders: an ever-expanding clinical spectrum, Front. Neurol. 12 (2021).

[56] Hooli, B.V., et al., PLD3 Gene Variants and Alzheimer's Disease. (1476-4687(Electronic)).
[57] Cruchaga, C., et al.,Rare Coding Variants in the Phospholipase D3 Gene Confer Risk for Alzheimer's Disease. (1476-4687 (Electronic)).
[58] Nackenoff, A.A.-O., et al., PLD3 Is a Neuronal Lysosomal Phospholipase D Associated with β-amyloid Plaques and Cognitive Function in Alzheimer's Disease. (1553-7404(Electronic)).
[59] G. Giachin, et al., Dynamics of human mitochondrial complex I assembly: implications for neurodegenerative diseases, Front. Mol. Biosci. 3 (2016) 33–43.
[60] M. Mimaki, et al., Understanding mitochondrial complex I assembly in health and disease, Biochim. Biophys. Acta 1817 (6) (2012) 851–862.
[61] Mosconi, L., M.J. Pupi A Fau - De Leon, and M.J. De Leon, Brain Glucose Hypometabolism and Oxidative Stress in Preclinical Alzheimer's Disease. (1749-6632 (Electronic)).
[62] D. Luque-Contreras, et al., Oxidative stress and metabolic syndrome: cause or consequence of Alzheimer's disease? Oxid. Med. Cell. Longev. 2014 (2014) 497802.
[63] J.R. Bamburg, B.W. Bernstein, Actin dynamics and cofilin-actin rods in alzheimer disease, Cytoskeleton (Hoboken) 73 (9) (2016) 477–497.
[64] S. Lye, et al., Exploring new avenues for modifying course of progression of Alzheimer's disease: the rise of natural medicine, J. Neurol. Sci. 422 (2021) 117332.
[65] B. Ding, et al., Gene Expression Profiles of Entorhinal Cortex in Alzheimer's Disease, 2014, pp. 1938–2731 (Electronic)).
[66] P.L. Zhenzhen Liu, Jiannan Wu, Yi Wang, Ping Li, Xinxin Hou, Qingling Zhang, Nannan Wei, Zhiquan Zhao, Huimin Liang, Jianshe Wei, The cascade of oxidative stress and tau protein autophagic dysfunction in Alzheimer's disease. Alzheimer's Disease - Challenges for the Future, 2015.
[67] Jr A. V. Terry, J.J. Buccafusco, The cholinergic Hypothesis of Age and Alzheimer's disease-related cognitive deficits: recent Challenges and their Implications for novel drug development, J. Pharmacol. Exp. Therapeut. 306 (3) (2003) 821.
[68] Dong, X.X., Z.-h. Wang Y Fau - Qin, and Z.H. Qin, Molecular Mechanisms of Excitotoxicity and Their Relevance to Pathogenesis of Neurodegenerative Diseases. (1745-7254(Electronic)).
[69] Liu, A.K., et al., Nucleus Basalis of Meynert Revisited: Anatomy, History and Differential Involvement in Alzheimer's and Parkinson's Disease. (1432-1533 (Electronic)).
[70] Abate, G., et al., The Pleiotropic Role of P53 in Functional/dysfunctional Neurons: Focus on Pathogenesis and Diagnosis of Alzheimer's Disease. (1758-9193 (Electronic)).
[71] M.-Y. Cha, et al., Mitochondrial ATP synthase activity is impaired by suppressed O-GlcNAcylation in Alzheimer's disease, Hum. Mol. Genet. 24 (22) (2015) 6492–6504.
[72] Bhatia, S., et al., Mitochondrial Dysfunction in Alzheimer's Disease: Opportunities for Drug Development. (1875-6190 (Electronic)).
[73] Shi, X., et al., Rat Hippocampal Proteomic Alterations Following Intrahippocampal Injection of Amyloid Beta Peptide (1-40). (1872-7972 (Electronic)).
[74] A. Misrani, S. Tabassum, L. Yang, Mitochondrial dysfunction and oxidative stress in Alzheimer's disease, Front. Aging Neurosci. 13 (2021) 617588.
[75] C. Guo, et al., Oxidative stress, mitochondrial damage and neurodegenerative diseases, Neural regeneration research 8 (21) (2013) 2003–2014.
[76] W.S. Liang, et al., Alzheimer's disease is associated with reduced expression of energy metabolism genes in posterior cingulate neurons, Proc. Natl. Acad. Sci. USA 105 (11) (2008) 4441–4446.
[77] I.L. Joo, et al., Early alterations in brain glucose metabolism and vascular function in a transgenic rat model of Alzheimer's disease, Progress in Neurobiology 217 (2022) 102327.
[78] M. Vanhoutte, et al., 18F-FDG PET hypometabolism patterns reflect clinical heterogeneity in sporadic forms of early-onset Alzheimer's disease, Neurobiol. Aging 59 (2017) 184–196.
[79] Tseng, H.C., et al. A Survey of Cdk5 Activator P35 and P25 Levels in Alzheimer's Disease Brains. (14-5793 (Print)).
[80] Lee, M.S., et al., Neurotoxicity Induces Cleavage of P35 to P25 by Calpain.(28-836 (Print)).
[81] T.J. Fukasawa, et al., CDK5 and MAPT gene Expression in Alzheimer's disease brain samples, Curr. Alzheimer Res. 15 (2) (2018) 182–186.
[82] Cenini, G. and W. VoosMitochondria as potential targets in Alzheimer Disease Therapy: an Update. (1663-9812 (Print)).
[83] Liu, H., M. Ye, and H. Guo An Updated Review of Randomized Clinical Trials Testing the Improvement of Cognitive Function of Ginkgo Biloba Extract in Healthy People and Alzheimer's Patients. (1663-9812 (Print)).
[84] Skvarc, D.R., et al.,The Effect of N-Acetylcysteine (NAC) on Human Cognition - A Systematic Review. (1873-7528 (Electronic)).
[85] McManus, M.J., J.L. Murphy Mp Fau - Franklin, and J.L. Franklin, The mitochondria-targeted antioxidant MitoQ prevents loss of spatial memory retention and early neuropathology in a transgenic mouse Model of Alzheimer's Disease. (1529-2401 (Electronic)).
[86] Shinn, L.A.-O.X. and S.A.-O. Lagalwar, Treating Neurodegenerative Disease with Antioxidants: Efficacy of the Bioactive Phenol Resveratrol and Mitochondrial-Targeted MitoQ and SkQ *LID - 10.3390/antiox10040573 [doi] LID - 573.* (2076-3921 (Print)).
[87] Reddy, P.H., M. Manczak, and R. Kandimalla, Mitochondria-targeted Small Molecule SS31: a Potential Candidate for the Treatment of Alzheimer's Disease (1460-2083 (Electronic)).
[88] Galimberti, D. and E. Scarpini, Pioglitazone for the Treatment of Alzheimer's Disease (1744-7658 (Electronic)).
[89] Biorender Available from: https://app.biorender.com/.